



# Controlled actuation, adhesion, and stiffness in soft robots: A review

Kunal Singh<sup>1</sup> · Shilpa Gupta<sup>2</sup>

Received: 26 March 2022 / Accepted: 7 October 2022 / Published online: 26 October 2022  
© Springer Nature B.V. 2022

## Abstract

Rigid robotic grippers are not capable of self-adjusting their grip size based on any real-time changes in the dimensions of the target object. This problem of self-adjustment can be addressed by soft robotic grippers. In the past few decades, new methods, and techniques to develop and control soft actuators have been explored by researchers worldwide. Soft robotic grippers can be categorized into three technologies which are controlled actuation, controlled adhesion, and controlled stiffness. Using these three technologies soft robots can mimic the morphology of the gripping and locomotion mechanisms of various animals. This study is aimed to present an introductory review for researchers who want to explore the field of soft robotics. While previous reports focussed on granular jamming structures to control stiffness, the present study emphasized laminar jamming structures and discussed the recent soft actuators developed using these structures. It was observed that soft actuators with a longitudinal strain like mckibben and peano HASEL exert high forces compared to bending actuators. Also, sandwiched laminar jammers can generate greater stiffness compared to homogeneous laminar jammers.

**Keywords** Soft robots · Soft robotics · Actuation · Adhesion · Stiffness · Jamming

## 1 Introduction

Traditional robotic grippers are made of rigid links which are highly accurate in adjusting their grip size as per the program or computer code. The rigid gripper attached to the free end of a manipulator is not capable of self-adapting its grip size based on any changes in the dimensions of the target object on the assembly line without any changes in the computer code or program which drives the manipulator. To solve this gripping problem, researchers have focused on the animal kingdom and tried to develop robotic grippers based on the morphology of animals [1]. Such grippers are designed using soft materials and actuated using unconventional smart materials. The advantage of such grippers is that the complexity of the control system is reduced due to mechanical compliance and material

softness [2]. By replacing rigid grippers with soft grippers on an industrial manipulator, the real-time ability of a robot to pick objects of different dimensions is enhanced. Soft robotic grippers or actuators are made of materials like elastomers [3], flexible shafts [4], polymers [5], and gels [6]. Unlike rigid grippers, the properties of the material used in the construction of a soft robot play an important role in the overall performance of the robot, therefore testing and simulation of such materials lay the foundation for the strength, motion, and energy needs of a soft gripper. Shintake et al. [7] presented three control technologies of soft actuators which are controlled through actuation, adhesion, and stiffness [7]. The reports gave a comprehensive overview of the material and mechanism of soft actuators [7]. The three control technologies are further subdivided based on the form of input energy required by an actuator, its material, and its mechanism. Researchers have even reported each technology separately. Fitzgerald et al. [8] presented the control of stiffness of soft actuators through jamming mechanisms [8]. Similarly, a study by Walker et al. [9] analyzed pneumatic soft actuators and their actuation behavior [9]. Adhesive properties of soft robots have also been separately presented by researchers. Boesel et al. [10] reported the fabrication methods and adhesive properties of gecko-inspired microfibrillar and

✉ Kunal Singh  
kunal7biz@gmail.com

<sup>1</sup> Department of Mechanical Engineering, Maharaja Agrasen Institute of Technology, Maharaja Agrasen University, Baddi 174 103, India

<sup>2</sup> Department of Electrical & Electronics Engineering, Maharaja Agrasen Institute of Technology, Maharaja Agrasen University, Baddi 174 103, India

nano fibrillar surfaces [10]. With recent advancements in composite materials, researchers are developing new methods and mechanisms to develop soft robots. These three control mechanisms are being combined to develop soft actuators with high strain, adaptable stiffness, and good surface adhesion.

The objective of this study is to explain the principle and operations of various soft actuators developed by researchers over the years under the three control technologies of soft robotics and compare their performances. The objective is to give the reader a thorough understanding of the three control technologies which may help to further improve the design of soft actuators. Section 2 classifies soft actuators based on the three control technologies which are further classified based on the energy sources required for actuation.

A simple tree structure is provided for the reader to understand the classification of control mechanisms and the input energy sources of these actuators. Section 3 explains the principle and operation of various soft actuators based on control actuation which includes pneumatic, McKibben, hydraulically amplifying self-healing electrostatic (HASEL), low voltage dielectric actuators (LVDEAs), and shape memory alloy (SMA) actuators followed by a thorough discussion comparing the performances of these actuators. Thereafter, Sect. 4 discusses the operation of soft actuators based on the controlled stiffness technique which includes granular jamming, laminar jamming, magnetorheological (MR), and low melting point alloy (LMPA) jamming followed by the discussion comparing the performances of these techniques, their advantages, and disadvantages. Section 5 discusses the operation of soft actuators based on electroadhesive and gecko adhesive techniques followed by a discussion comparing these techniques, their advantages, and disadvantages. Section 6 of this article, discusses the future challenges explaining the advantages and disadvantages of various actuators and the research required to improve the performance of these actuators, their advantages, and disadvantages. Section 7 summarized the performance of various soft actuators quantitatively.

Previous studies focussed on stiffness control through granular jamming, therefore in this article discussion of some recent advancements in the laminar jamming mechanism to control stiffness is also done apart from granular jamming. This article provides a discussion on some recent actuators developed using homogeneous, discrete, and sandwiched laminar jamming techniques. It was observed through the comparison of performance parameters that McKibben actuators, peano HASEL actuators, and MR jammers can exert high forces, while sandwiched laminar jammers can generate high stiffness forces compared to homogeneous laminar structures.

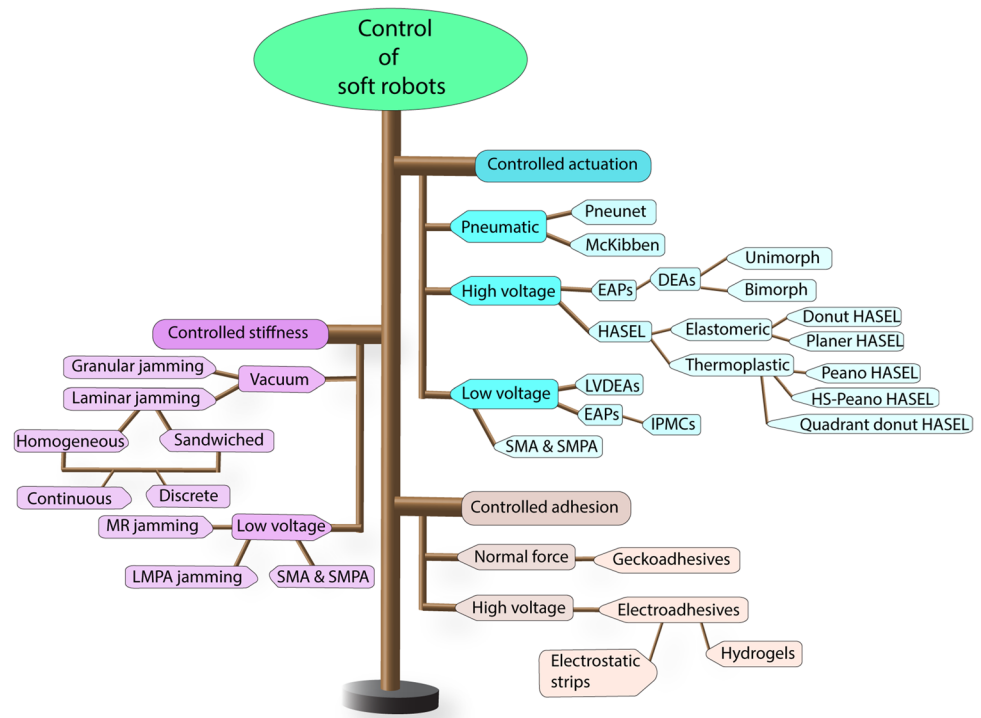
## 2 Classification of soft actuators

Soft robotic grippers when categorized based on the control mechanism can be of three types a) controlled actuation [2] b) controlled stiffness [11], or c) controlled adhesion [12]. These three technologies are mostly used in combination to develop a soft actuator or gripper. Figure 1 displays the tree structure of various soft robot control technologies developed under these three categories. Actuation or motion can be controlled using three sources of power which are pneumatic pressure [13], high voltage [14], and low voltage [15]. Two types of soft actuators driven by pneumatic energy are pneumatic [16] and McKibben [17] actuators. High voltage actuators include electro-active polymers (EAPs) [5] like dielectric elastomer actuators (DEAs) [18] which are further classified as unimorph and bimorph based on the capability to bend in one or two directions. High voltages also drive HASEL [19] actuators. Actuators under the low voltage category include LVDEAs [15] and electro-active polymers like ionic polymer metal composites (IPMCs). Controlled stiffness generally can be achieved using vacuum energy or with the application of low voltages. Granular jamming [8] and laminar jamming [20] are two popular methods to control stiffness that require a vacuum source to activate. Laminar jamming structures can be homogeneous [21] or non-homogeneous [22] (also called “sandwiched”). Further, both homogeneous and sandwiched laminar jammers can be categorized as continuous or discrete based on the condition of whether friction force in the laminar structure is acting throughout the layers or discretely at some sections. Low voltage stiffness includes MR jammers [23], LMPA jammers [24], and SMA & SMPA [25] based stiffening actuators. Lastly, the adhesion of soft robots can be controlled by the application of normal force [26] (which exploits the use of frictional forces and weak Vanderwall forces) and the use of high voltages [27]. Geckoadhesive technology [28] for soft robots is inspired by observing mother nature’s creations such as lizards and other geckos who can climb walls with the help of millions of microscopic hair-like structures on their foot. High voltage adhesives include the use of electrostatic strips [29] and hydrogels [30]. The principle of operation & applications of some of these technologies are discussed in detail in further sections. It may also be noted that the techniques introduced in Fig. 1 may not be the only available methods to control soft robots, as the field is very extensive, and continuous research in this field is exploring new methods to control soft robots.

## 3 Controlled Actuation

Actuation relates to the motion of a soft actuator. The effective control of the movement or strain of the soft robot is essential to interact with the environment. Controlling the

**Fig. 1** Tree of soft robots displaying various control mechanisms and their energy sources



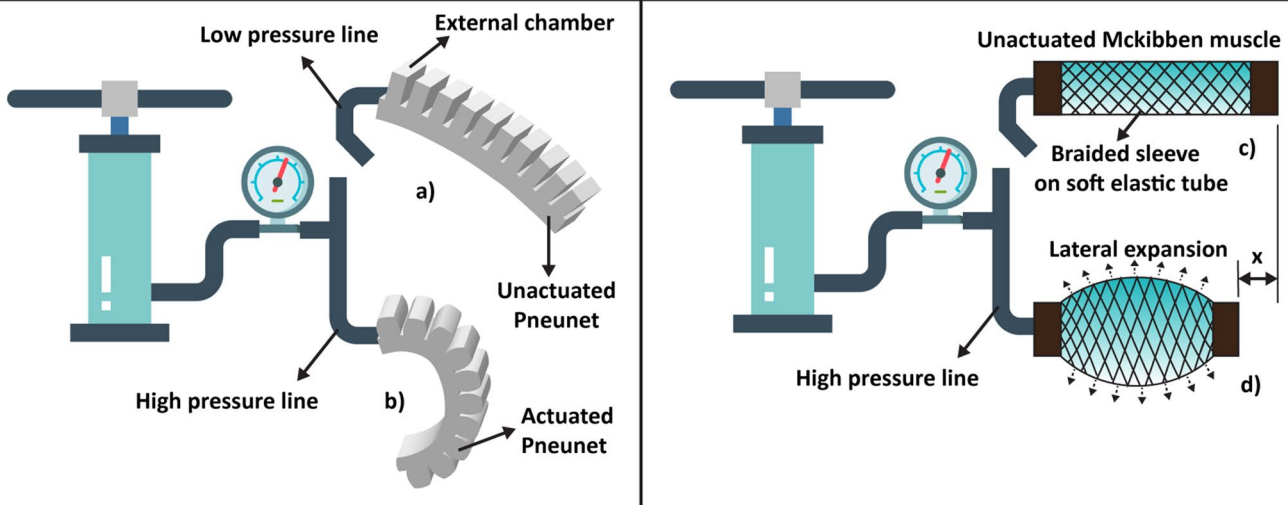
movement of a soft gripper depends on the shape, size, and material of the gripper. Unlike traditional robotics where motors of various kinds (Brushless, Servo, Stepper, DC, AC) are used for the actuation of a joint, in soft robotics, other methods and materials for actuation are used such as soft pneumatic structures [31], dielectric elastomers [32], shape memory alloys (SMAs) & polymers (SMPs) [33], electrostatics [34], etc. Soft pneumatic actuators can be broadly subdivided further into pneunet actuators and mckibben actuators.

### 3.1 Controlled actuation through pneumatics

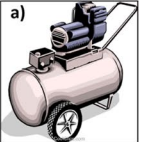
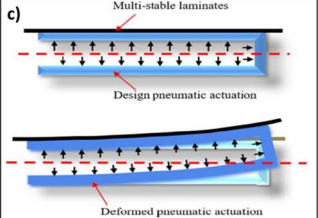
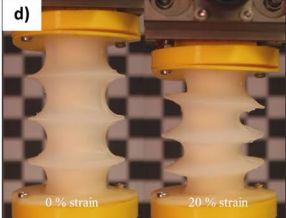
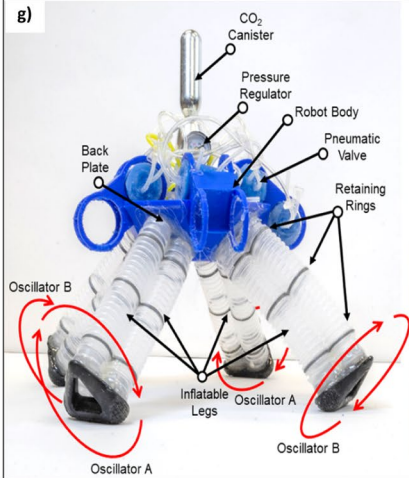
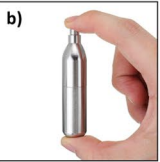

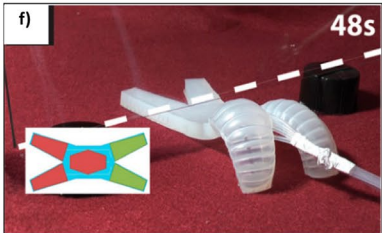
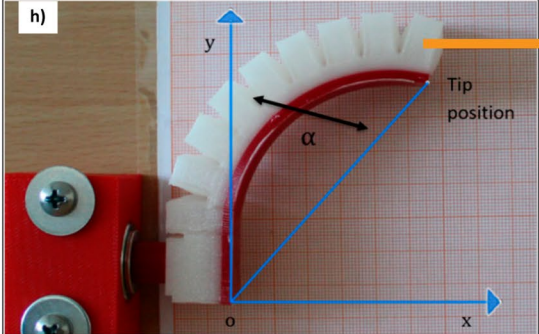
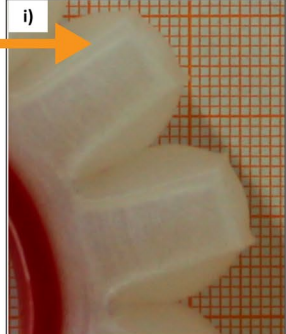
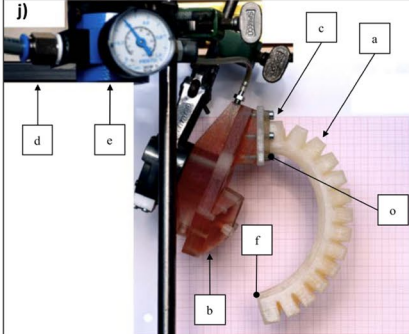
As shown in Fig. 2a, pneunet is a pneumatic actuator made of soft compliant material like rubber, silicone, thermoplastic polyurethane (TPU), or any other material with hyper-elastic or elastic properties. The shape and material of the pneunet determine the amount of actuation and pressure requirement. Under low pressure, pneunet is not actuated, and the only possible bending observed is due to the gravitational force in this cantilever configuration. Under fluid pressure, the pneunet actuates Fig. 2b and bends due to its asymmetric geometry and relative expansion of thin wall surfaces compared to the thick base. McKibben muscle or actuator consists of a soft elastic tube inside a braided mesh tube as shown in Fig. 2c. One end of the mckibben actuator is sealed and the other connects the pneumatic pressure line. Under fluid pressure, the mckibben muscles Fig. 2d expand laterally and contract in the longitudinal direction.

The braided sleeve assists this lateral expansion and longitudinal contraction.

The applications of pneunet actuators range from the food industry to prosthetics. A group of researchers developed a hybrid gripper for the food industry with pneunet fingers and the suction cup on the fingertips [35]. The gripper was able to lift a “MacBook Air” weighing more than 1 kg using this hybrid gripper [35]. The advantage of using soft grippers in the food industry is the added effectiveness to lift soft compressive objects of various sizes. Figure 3a and 3b display the energy source for a soft pneumatic actuator. Any fluid with the capability to exert pressure can be used for the actuation of soft pneumatic robots. Soft actuating grippers are often integrated with jamming structures to increase their rigidity. Pneumatic actuators can be integrated with multistable laminate structures as shown in Fig. 3c to provide large deformations and improve the rigidity of the structure [31]. Figure 3d displays a vacuum-powered ultra-light PAM (Pneumatic Actuated Muscle) having a bellow configuration integrated with rings at each convolution which increased the buckling load of the actuator [36]. Soft actuators can be cast, or 3D printed, 3D printed actuators bear considerably less elongation than cast material [37]. The rotational casting method can be employed to develop soft actuators, using this method a wearable assistive device for rehabilitation purposes was developed as shown in Fig. 3e [38]. Apart from grippers walking soft robots are also an area of interest, As shown in Fig. 3f researchers designed a multi-gait robot using soft elastomer and fluid



**Fig. 2** Operation of pneumatic and mckibben actuators: (a) unactuated pneumatic actuator; (b) actuated pneumatic actuator; (c) unactuated mckibben actuator; (d) actuated mckibben actuator

| Energy source  | Controlled actuation using pressure   |  |   |
|--|---|--|---|
| <p>Compressed air from air compressor</p>  <p>a)</p>                       |  <p>c)</p>  |  <p>d)</p>  |  <p>e)</p>  |
| <p>Expanding gas example CO<sub>2</sub> or pressurized gas</p>  <p>b)</p> |  <p>e)</p> |  <p>f)</p> |   |
|  |  <p>h)</p> |  <p>i)</p> |  <p>j)</p> |

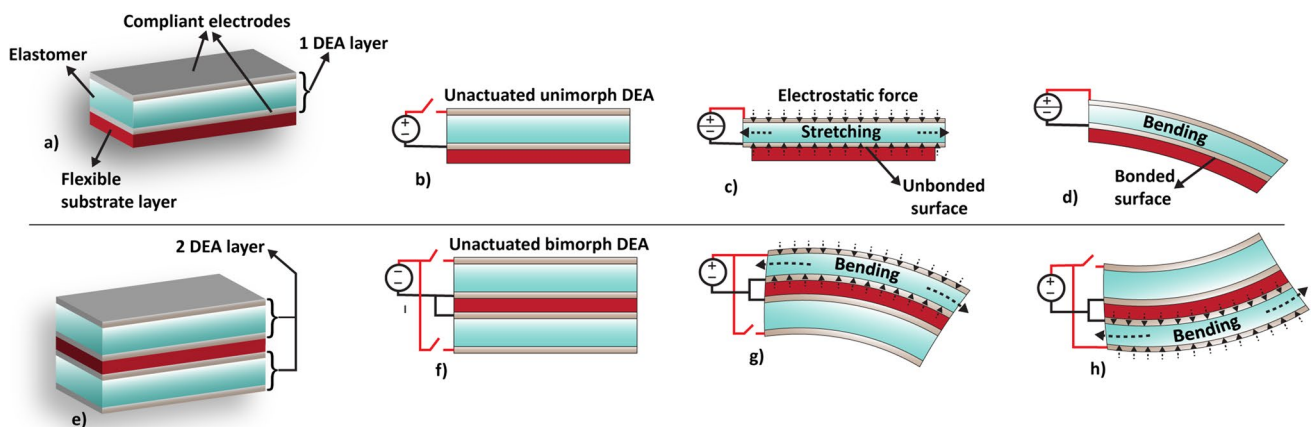
**Fig. 3** Controlled actuation of soft actuators using pneumatic pressure: (a) air compressor as an energy source; (b) compressed gas as a portable energy source; (c) pneumatic actuator with multistable laminate structures [31]; (d) ultralight pneumatic actuator (PAM) [36]; (e) wearable assistive pneumatic actuator [38]; (f) multi-gait soft robot

[39]; (g) electronics-free pneumatic robot [40]; (h) R type MBP under actuation [41]; (i) behavior of R type MBP outer walls under pressure [41]; (j) experimental setup to determine the bending behavior of silicone-based 3D printed pneumatic [37]

actuation. The developed robot require low pressure ( $< 10$  psi) to actuate and was capable of walking in a gravitational field without an internal and external hard skeleton [39]. Researchers are also developing robots that do not require electronics but are driven completely using pneumatic circuits, Fig. 3g displays one such robot, the locomotion of this robot is efficient, fluent, and quite natural [40]. The disadvantage of such a robot is the dependency on the available quantity of compressed gas cylinders, which also reduces the performance (walking speed, response time) of robots as the level of gas decreases. Some researchers have also constructed different designs of monolithic bending pneunets (MBPs) which were 3d printed using the fused filament fabrication (FFF) technique [41]. In their studies, different grades of TPU (shore hardness 95 and 80) were used to fabricate inextensible and extensible segments of MBPs and, observations were made that the improved R-type actuator has the best performance and achieved a bending angle of  $72.9^\circ$  with 4 bar of applied pressure [41]. Figure 3h displays the bending of R-type MBP under air pressure, and Fig. 3i displays how the outer walls of R-type MBP exert pressure on each other to create the bending shape. Another group of researchers studied the performance of a 3d printed pneunet made from silicone [37]. In their studies, observations were made that due to the inhomogeneity of 3D printed pneunet, it allows less elongation compared to cast pneunet and, simulation of the model using the YEOH model showed a 10% deviation from the actual deformations achieved in the experiments [37]. Figure 3j displays the experimental setup to estimate the bending behavior of pneunet under various pressures [37].

### 3.2 Controlled actuation through DEAs & SMAs

Electroactive polymers [42] like dielectric elastomers actuators (DEA) deform when a high voltage electric field is applied to them. Figure 4a displays a unimorph dielectric actuator, the active DEA layer consists of an elastomer sandwiched between two compliant electrodes. Figure 4b shows the unactuated unimorph DEA actuator with its connections to the high voltage power supply. Figure 4c displays the state of DEA when high voltage is provided to electrodes. The elastomer is compressed due to electrostatic attraction between the electrodes which stretch the elastomer, In Fig. 4c the DEA layer is not bonded to the substrate layer which is not elastic but flexible enough to bend with the DEA layer. But when the DEA layer is bonded to the substrate layer as shown in Fig. 4d then the cantilever structure bends due to uneven stretching of the elastomer. The bonded surface of the DEA layer to the substrate prevents the elastomer from stretching in the lower region but it is free to stretch in the upper region which causes bending. Figure 4e displays the bimorph [18] configuration of DEA in which the substrate is sandwiched between two DEA layers. In this case, as shown in Fig. 4f there are four electrodes, two for the upper DEA layer and two for the lower DEA layer connected to a high voltage power supply. When high voltage is supplied to the electrodes of the upper DEA layer as shown in Fig. 4g a hogging effect is produced in this bimorph beam. Bimorph structure is bidirectional and when the lower DEA layer is actuated as shown in Fig. 4h it bends in another direction.

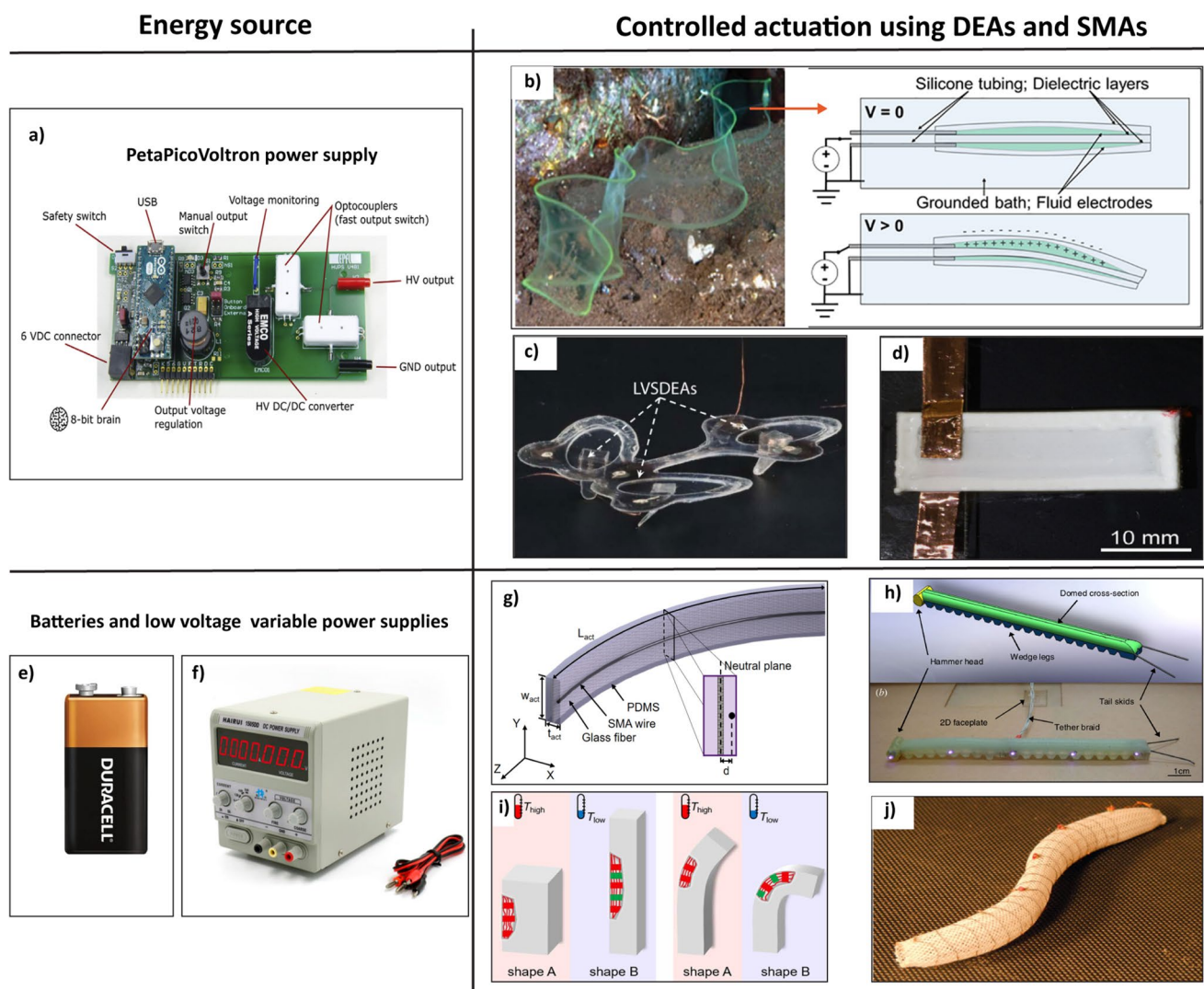


**Fig. 4** Actuation states of dielectric actuators: (a) structure of unimorph DEA; (b) unactuated unimorph DEA connection with high voltage supply; (c) actuation state of unbonded unimorph DEA; (d) actuation state of bonded unimorph DEA; (e) structure of bimorph

DEA; (f) unactuated bimorph DEA connection with high voltage supply; (g) hogging state in bimorph DEA; (h) sagging state in bimorph DEA

A neon transformer can be used to power DEAs which convert line voltage to high voltage ranging from 2 to 15 kV. Rectification and control of current are some of the requirements at its output before the generated high voltage can be used to actuate the dielectric actuator. Another good source of power for DEAs can be a low current high voltage power supply like the open-source Arduino-based supply called “PetaPicoVoltron” [43] as shown in Fig. 5a. DEAs may require high voltages such as 7.5 kV to generate the required bending as shown in Fig. 5b [32], but very high voltage is not always necessary. Researchers have developed small-scale (1 g in weight, 4 cm long) untethered autonomous robots driven by low voltage stacked dielectric elastomers (LVSDEAs) shown in Fig. 5c [44]. The driving voltage

to actuate this robot was below 450 V with an operational frequency of around 600 Hz. Certain features of LVSDEAs such as low driving voltage requirement along with high power density make them suitable to be used as artificial muscles to drive such miniature robots. Another way of controlling the actuation of a soft robot is by integrating it with shape memory alloys (SMAs). The property of SMAs to retain shape when heated within a range of temperature make them suitable for producing complex movements in a soft robot. SMAs remember their shape in the austenite phase. In the martensite phase, SMA can be deformed to any shape. An efficient way of using SMAs in soft robots is to provide energy in the form of electricity to these alloys instead of external heating. Due to internal resistance and



**Fig. 5** Controlled actuation in DEA and SMA-based actuators: (a) “PetaPicoVoltron” open-source power supply to actuate DEAs [43]; (b) high voltage dielectric actuator [32]; (c) mini robot based on low voltage dielectric actuators (LVDEAs) [44]; (d) 3D printed unimorph DEA [42]; (e) 9-V battery as an energy source for SMA-based actuators;

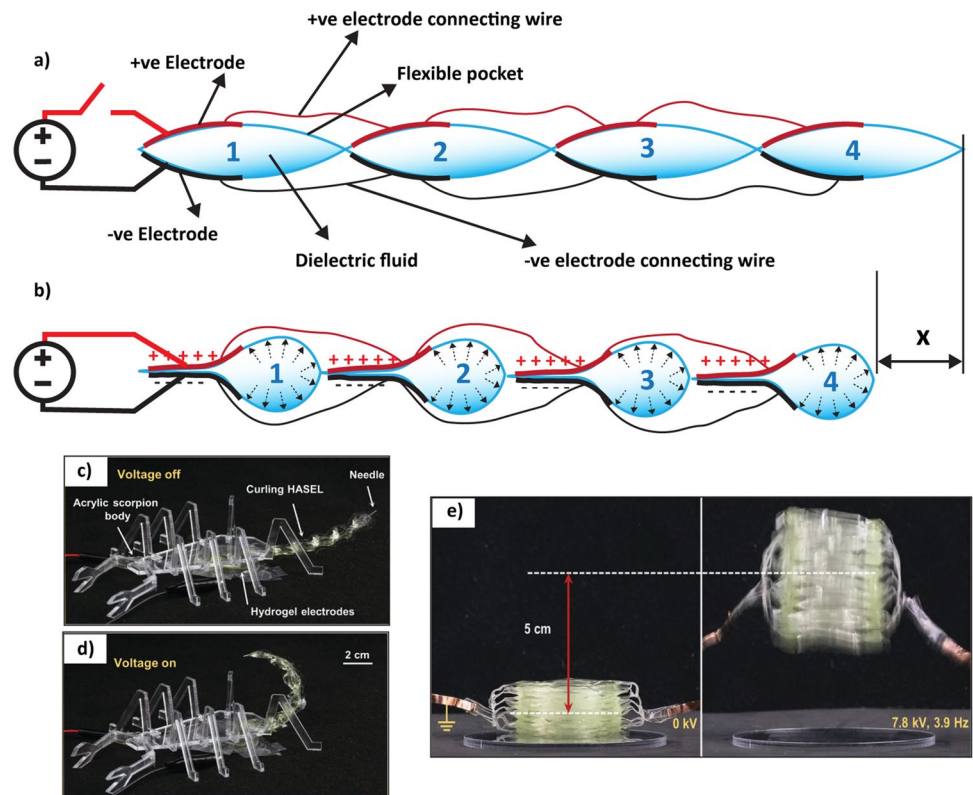
(f) variable DC power supply for SMA-based actuators; (g) SMA integrated with PDMS actuator [33]; (h) caterpillar-inspired soft robot [45]; (i) states of a soft actuator based on reprogrammable shape memory alloy [46]; (j) meshworm: SMA-based worm-like robot with peristaltic motion [47]

hence heat generation phase is transformed from martensite to austenite where SMA changes its shape. Figure 5d shows a unimorph configuration of DEA developed by researchers through 3d printing technology. This DEA [42] is constructed from ionic hydrogel elastomer hybrid material and was able to achieve a maximum tip deflection of  $9.78 \pm 2.52$  mm at 5.44 kiloVolts. Figure 5e-f shows the possible energy source to power SMA-based actuators. It can be a simple 9-V battery or a variable power supply. As shown in Fig. 5g an actuator developed by researchers was made from a PDMS (Polydimethylsiloxane) matrix integrated with flexinol/dynalloy SMA wire having a diameter of  $203.2 \mu\text{m}$  [33]. Figure 5h shows a soft robot developed by researchers based on the morphology of a caterpillar. The robot consists of a flexible body made from silicone integrated with SMA wires for actuation. The developed robot was able to perform rolling action like a caterpillar with an acceleration of 1 g and more than 200 rpm of angular velocity [45]. Some researchers proposed a reprogrammable SMPA (Shape memory polymer actuator) which can be reprogrammed to achieve desirable deformation [46]. The proposed design was constructed from a blend of copolymers which is shown in Fig. 5i [46]. Researchers also developed a structure with artificial circular and longitudinal muscles made from NiTi (nickel-titanium) coiled wires [47]. The antagonistic arrangement of muscles aided the peristaltic motion of this worm-shaped mechanism named “meshworm” [47] as shown in Fig. 5j.

### 3.3 Controlled actuation through HASEL actuator

Controlled actuation can also be achieved using a combination of electrostatics with the action of compressed fluid in a sealed flexible pocket. Such actuators are called Hydraulically amplified self-healing electrostatic lightweight actuators (HASEL). These actuators are lightweight and inexpensive and can exert large forces compared to their weight. Figure 6a displays the construction of a HASEL actuator. These actuators consist of a series of dielectric fluid-filled pockets made of flexible material. Some portions of the outer periphery of these pockets are bonded with flexible electrodes. When a high voltage electric field is applied to the electrodes, due to electrostatic attraction the flexible membranes of fluid-filled pockets are compressed, and due to internal pressure, the other half of the pocket tries to achieve a spherical shape as shown in Fig. 6b. Due to this a contractive force is exerted in the longitudinal direction, the larger the number of pockets, the more will be the contraction. Figure 6c and d display an artificial scorpion in an un-actuated state. When voltage is applied this tail can achieve a striking velocity of  $1.26 \text{ m s}^{-1}$ , which resembles the striking velocity of an actual scorpion [19]. Figure 6e shows the stack of donut-shaped HASEL actuators performing a jump when 7.8 kV is applied to it at a 3.9 Hz frequency [19]. It may be observed that HASEL actuators due to their high force to

**Fig. 6** Controlled actuation through HASEL actuators: (a) unactuated state of HASEL actuator; (b) actuated state of HASEL actuator; (c) unactuated state of HASEL actuator on an acrylic scorpion body [19]; (d) actuated state of HASEL actuator on an acrylic scorpion body [19]; (e) donut-shaped HASEL actuators performing a jump [19]



mass ratio and quick response time are good at mimicking the dynamic actions performed by animals and humans.

### 3.4 Comparison of soft actuators based on controlled actuation

Table 1 compares the soft actuators driven by energy sources like pneumatic pressure and high and low voltages. It may be observed that pneumatic actuators are typically large compared to dielectric actuators, also pneumatic actuators can exert significantly large forces as compared to dielectric actuators. This is because fluid pressures have a greater tendency to resist opposing forces. As can be observed from Table 1, McKibben actuators can exert high forces when compared to pneunet, and forces generated by peano HASEL actuators [48] are comparable to McKibben actuators [49]. This is because the mechanism of operation of peano HASEL and McKibben actuators are somewhat similar. The excess fluid pressure exerted on the inside walls of peano HASEL actuators which produces a compressive strain is similar to the action of air pressure exerted on the inside walls of McKibben actuators. In both types of actuators, lateral fluid pressure produces longitudinal compressive strain.

It may be noted that the deflection in actuators like pneunets, unimorph DEAs, bimorph DEAs, LVDEAs, and IPMCs is generally bending type while actuators like McKibben and peano HASEL bear the linear compressive strain as discussed above. The bending behavior is due to the presence of longitudinal layers with uneven properties in all such actuators. In the case of pneunet, the structural change in the

bottom and top portions can be observed. The top portion is expandable using fluid pressure while the bottom bonded portion is non-expandable. Similarly, in the case of DEAs, the top portion can be stretched using electrostatic actuation, while the bottom bonded portion is flexible but not stretchable.

It may be concluded that soft actuators with longitudinal strain whether directly or indirectly actuated by fluid pressure (McKibben actuators directly driven, peano HASEL indirectly driven) produce much higher resistive force compared to bending actuators like pneunet, DEAs, LVDEAs, or IPMCs. Table 1 provides a general overview of some of the key performance parameters based on some published results for grippers or actuators driven for controlled actuation. The values in Table 1 do not represent the ultimate performance of such actuators but provide some quantified means for comparison. The range of forces generated by pneumatic, dielectric, and SMA & SMPA based actuators are compared in Fig. 7 which depicts that peano HASEL and McKibben actuators produce much higher forces.

From Fig. 8 it may be concluded that the input high voltage required by peano HASEL actuators is also large around 8 kV compared to other high voltage actuators which may be attributed to the fact that HASEL actuators require a much higher electrostatic charge to compress the fluid pocket that generates high longitudinal compressive force.

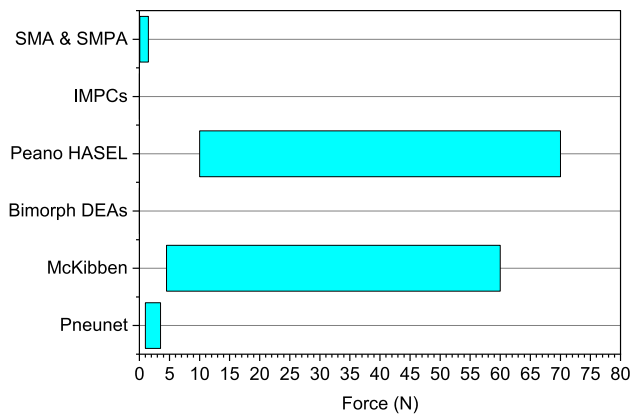
Advantages and disadvantages of soft actuators based on controlled actuation.

Reports indicate that large bending deformations can be produced at low pressures using pneunet actuators, similarly,

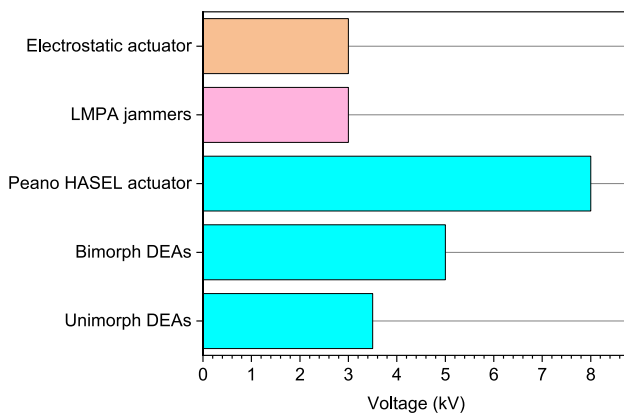
**Table 1** Comparison of the performance parameters of various soft actuators that are governed through controlled actuation

| Energy source | Actuator Type         | Effective Actuator length (mm) | Deflection (mm) /Angle (deg.)/ Strain           | Supplied power/ pressure /voltage/ Current | Resistive force (N)/ Stiffness (N/m) | Response time (s)       | Surface Condition (Wet/Dry) |
|---------------|-----------------------|--------------------------------|---|--|--------------------------------------|-------------------------|-----------------------------|
| Pneumatics    | Pneunet actuator      | 70 to 150 [16, 35, 37, 41]     | 90 to 130 mm [16, 37, 41], 70 <sup>0</sup> [35] | 24 to 400 kPa [16, 35, 37, 41]             | 1 to 3.5 N [16, 35]                  | 1 to 2 [16, 35, 37, 41] | dry [16, 35, 37, 41]        |
|               | McKibben actuator     | 180 to 300 [49–51]             | 9 mm [49], 10 to 27% [50, 51]                   | 50 to 550 kPa [49–51]                      | 4.5 to 60 N [49–51]                  | 1 to 5 [49–51]          | dry [49–51]                 |
| High voltage  | Unimorph DEAs         | 20 to 60 [52, 53]              | 1.5 to 6.5 mm [52, 53]                          | 3 to 3.5 kV [52, 53]                       | –                                    | –                       | dry [52, 53]                |
|               | Bimorph DEAs          | 20 to 60 [54, 55]              | 6 to 6.5 mm [54, 55]                            | 3 to 5 kV [54, 55]                         | 0.003 N [55]                         | 6 [54]                  | dry [54, 55]                |
| Low voltage   | Peano -HASEL actuator | 3 to 120 [48, 56]              | 10 to 15% [56], 14 mm [48]                      | 6 to 8 kV [48, 56]                         | 10 to 70 N [48, 56]                  | 5 to 10 [48, 56]        | dry [48, 56]                |
|               | LVDEAs                | 40 [44]                        | 45 <sup>0</sup> [57], 110 μm [44]               | 6 V [57], 450 V [44]                       | –                                    | 0 to 50 [57], >0.2 [44] | dry [44, 57]                |
|               | IPMCs actuator        | 80 [58], 20 [59]               | Exceeds 180 <sup>0</sup> [58],                  | 1 to 4 V [58],                             | ~0.016 N [58]                        | 2 [58]                  | dry [58]                    |
|               | SMA & SMPA actuator   | 100 to 130 [33, 60]            | 90 <sup>0</sup> to 180 <sup>0</sup> [33, 60]    | 1A [33, 60]                                | 0.08 to 1.5 N [33, 60]               | 5 to 75 [33, 60]        | dry [33, 60]                |





**Fig. 7** Comparison of range of forces generated by pneumatic, dielectric, and shape memory alloys and polymer-based actuators



**Fig. 8** Comparison of high voltage actuators in terms of input voltage requirement

such large deformations can be obtained using DEAs at very low power consumption, but high voltages. Also, McKibben and HASEL actuators can generate high uniaxial forces. The modular nature of HASEL actuators is an added advantage because individual elements of HASEL can be attached in series to generate large strains with high forces.

But even though pneunet's, DEAs, LVDEAs, and IMPC actuators can generate large deformations, their bending stiffness is very low. The use of high voltages in actuators like DEAs and HASEL makes the system bulky and relatively dangerous. The requirement of large input pressures to generate good uniaxial forces in McKibben actuators is an added disadvantage.

### 3.5 Controlled Stiffness

Apart from actuation of the gripper, stiffness can be utilized to grasp objects, in this case, shape memory alloys & shape memory polymers can be used to control the stiffness by

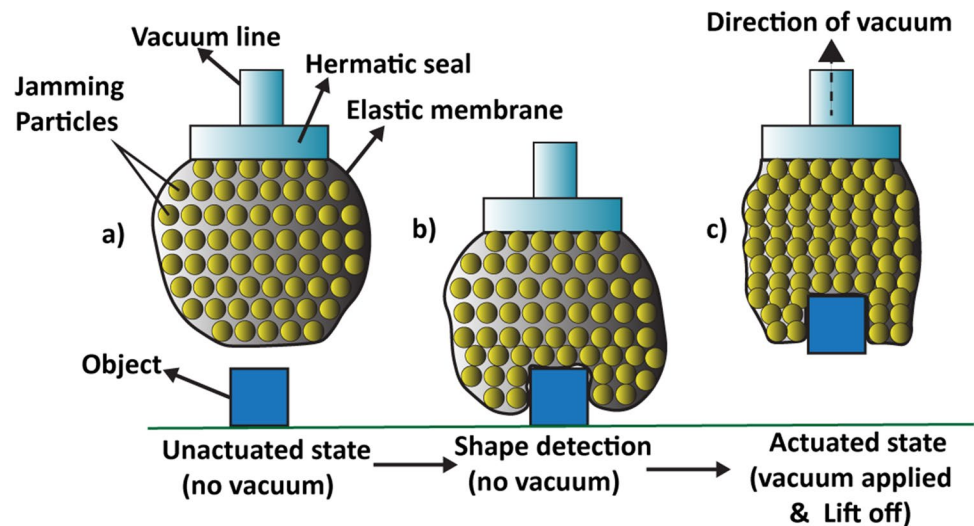
exploiting the flexibility of its soft state to reach the desired position and then using its rigidity to achieve the forces required [7, 11, 61]. The stiffness of a soft robot can also be controlled by exploiting the fluid properties and change in the state of certain materials like magnetorheological (MR) fluid [23], Low melting point alloy [24, 62, 63], or a combination of both which react to electric and magnetic fields [7, 8]. Granular jamming is another method to control the stiffness of a soft robot. The physics behind granular jamming is to solidify the state of particles filled in a flexible, elastic membrane structure by reducing the space between the particles. Such jamming is mostly achieved simply by creating a vacuum inside the particle-filled elastic bag or pouch.

### 3.6 Controlled stiffness through granular jamming

Figure 9 compares the process of granular jamming with MR fluid jammers. The structure and operation may seem similar but the physics behind these jammers is different. Broadly there are 3 steps involved in these grippers, which are required to lift an object effectively. These steps are 1) Unactuation, 2) Shape adjustment, and 3) Actuation. Figure 9a displays the granular jammer in an unactuated state where no vacuum is applied and all the particles inside the elastic membrane are loosely packed. Figure 9b shows the shape adjustment state in which the granular jammer is still unactuated, but it tries to adjust its membrane shape due to the compressive force given by the object. Figure 9c displays the third step in which a vacuum is applied to the jammer and particles tightly pack and generate a rigid structure suitable for good grip.

Researchers have created jamming structure with all sorts of granular material, such as with coffee powder [64–68], corn [69], crushed coffee [70], glass spheres [71–80], gravel [66], ground coffee [70, 72, 81–94], plastic cubes [95, 96] & spheres [66, 69, 85, 95–99], polystyrene [70, 100], wooden cubes [100], rubber cubes [95, 101, 102] and even materials like rice [66, 103], salt [83] and sugar [83, 104]. Figure 10a displays a granular jammer on a mobile robot. Researchers used crushed coffee, ground coffee, and Styrofoam of 2.5 mm and 1.2 mm size as the jamming particles. It was observed that small granular particles based jammer can exert high grasping force [70]. Figure 10b shows a granular jamming structure that works on the principle of the variable inner volume. A powder layer was introduced by the researchers in between two silicon layered structures of the gripper. This arrangement reduced the amount of powder and pushing force required for grasping [65]. Some researchers also developed a soft actuator with an integrated granular jamming layer as shown in Fig. 10c. In the proposed structure corn was used as the jamming particle. In this parallel jammer and actuator arrangement, the stiffness was controlled by granular jamming while air

**Fig. 9** Operation of the granular jamming structure: (a) granular jammer in unactuated state; (b) state of shape detection by the granular jammer; (c) granular jammer activated using vacuum, space between particles is reduced and grip is obtained



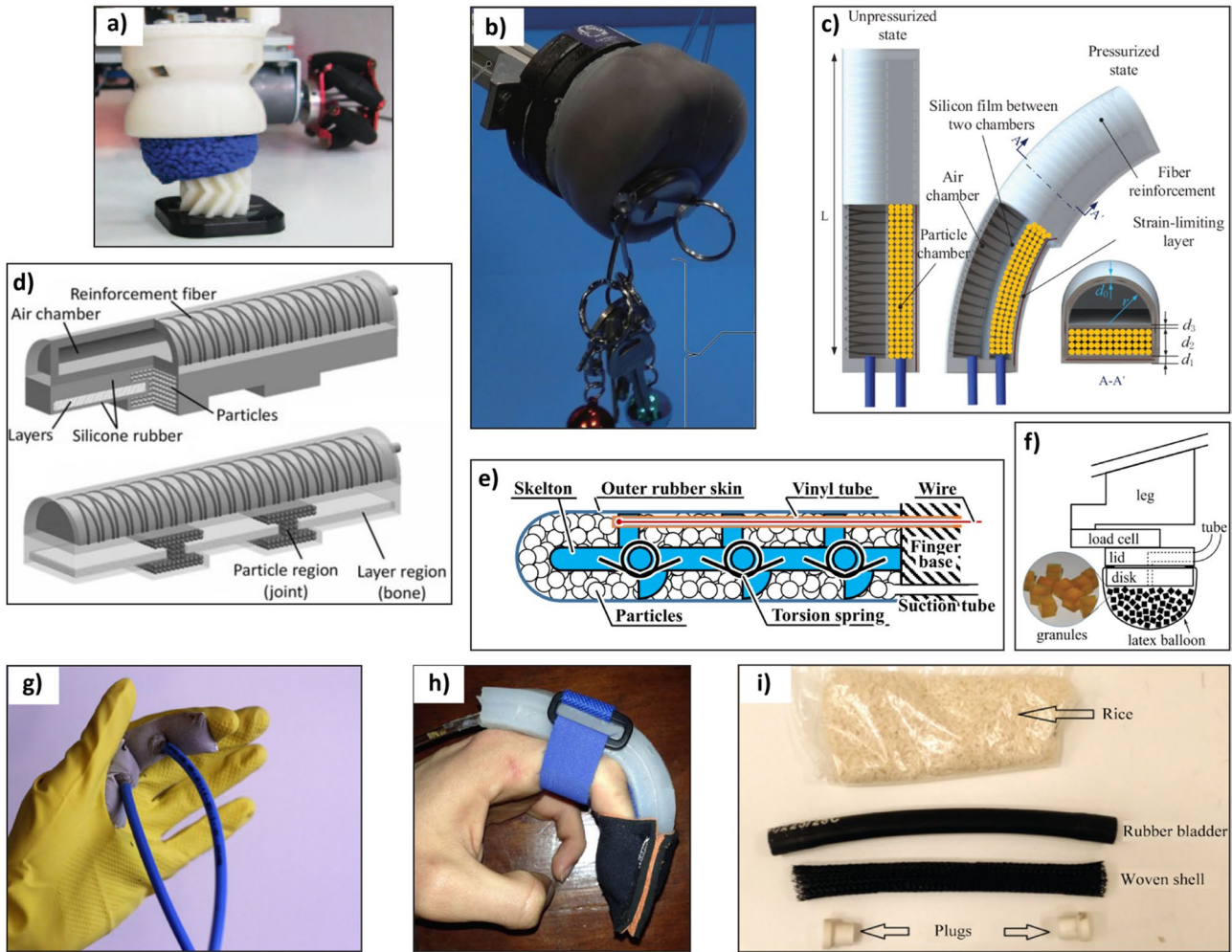
pressure was used for the movement of the structure [69]. Jamming structures can also be employed to effectively control the stiffness of a particular region in an actuator like controlling the stiffness of joints of an artificial soft finger. Figure 10d displays a robotic finger with a hybrid jamming structure employed at the joints and a layer jamming structure at the linkages. By controlling the vacuum supplied to the layer jamming and particle jamming structures a range of stiffnesses were obtained. Glass particles of 2 mm diameter were used for particle jamming in this gripper [79]. The process of layer jamming will be discussed further. As shown in Fig. 10e researchers have developed a multi-fingered gripper with torsion springs installed at the joints placed inside the rubber skin filled with granular material to generate stiffness. The actuation was performed using a wire attached to the inner skeleton of the finger. Coffee powder, beads, rice, and gravel were used as granular material [66]. Granular jamming can also improve the motion of a robot. Researchers investigated the use of granular jamming grippers for efficient locomotion of a quadruped robot as shown in Fig. 10f [102]. The reports suggested that the use of a jamming mechanism assisted to create a soft fluid state in the feet to damp impact forces along with a hard state for efficient propulsion [102]. As per the reports, the use of jammers also allowed the robot to climb steep surfaces at a faster rate [102]. Figure 10g displays a haptic glove developed by researchers for telemanipulation purposes. The glove can be used to sense virtual devices by providing resisting stiffness to fingers using jamming tubes or jamming pads. The proposed glove was able to resist forces up to 7 N with 5 mm displacement in jamming structures [100]. An exoskeleton was also developed by researchers as shown in Fig. 10h for hand operations based on granular jamming. It was developed for rehabilitation purposes and experiments and simulations were performed to analyze the

relation between jammer size and resistive force or bending stiffness generated within the jammer [104]. Researchers developed a jamming structure made of a rubber tube filled with rice [103]. Figure 10i displays the components of the structure. The proposed structure consists of a soft finger made of three pneumatic muscles integrated with this granular structure [103]. The studies showed that even with such a simple configuration the bending stiffness of a soft finger can be increased from 21 N/m to 71 N/m.

### 3.7 Controlled stiffness through laminar jamming

The process of controlling stiffness through laminar jamming in soft robotics is recently being explored by researchers due to its simple and effective operation. In this process, a stack of sheets of thin material (Paper, plastic, etc.) is sealed inside an airtight plastic or silicone covering. Originally this stack of paper is quite flexible and able to bend easily as sheets slide onto each other when bending is applied, but under a vacuum, it forms a rigid structure acting like a solid beam due to friction between the layers. Way before the field of soft robotics even emerged researchers exploited the principles of laminar jamming to develop variable stiffness devices. Researchers developed devices with stacked layers of flexible polyimide films sandwiched between patterned Ni electrodes as shown in Fig. 11a [105]. With the application of high voltages, the electrodes generate a compressive force on flexible films to produce the laminar jamming effect. Researchers developed actuators consisting of 12 layers of acrylic sheets with teeth-like structures (200  $\mu\text{m}$  thickness  $\times$  15 mm width  $\times$  50 mm length) micromachined on them as shown in Fig. 11b [106]. With the application of vacuum pressure, the structure produced the laminar jamming effect. Researchers developed a multi-layered beam structure made from PMMA (polymethyl methacrylate) with

## Controlled stiffness using granular jamming

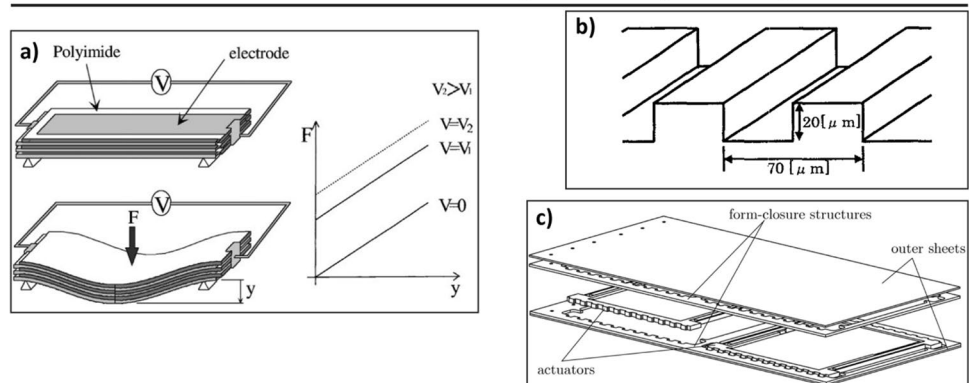


**Fig. 10** Controlled stiffness using granular jamming structures: (a) jamming gripper on a mobile robot [70]; (b) granular jammer made using the principle of the variable inner volume [65]; (c) granular jammer integrated with pneumatic actuator [69]; (d) a hybrid laminar and granular jamming structure [79]; (e) granular jammer integrated with soft robotic finger actuated using wire [66]; (f) granular

jammer with rubber cubes integrated at the feet of a quadruped robot [102]; (g) a telemanipulation glove with granular jammer filled with polystyrene beads [100]; (h) a rehabilitation device with a granular jammer [104]; (i) components of a simple granular jamming structure with rice as jamming particles [103]

**Fig. 11** Early attempts on creating laminar jamming structures: (a) laminar jamming structure made from layers of polyimide films between NI electrodes [105]; (b) dimensions of the comb-type layer of a laminar structure [106]; (c) PMMA laminar structure with dielectric elastomers for controlling stiffness [107]

## Controlled stiffness using laminar jamming

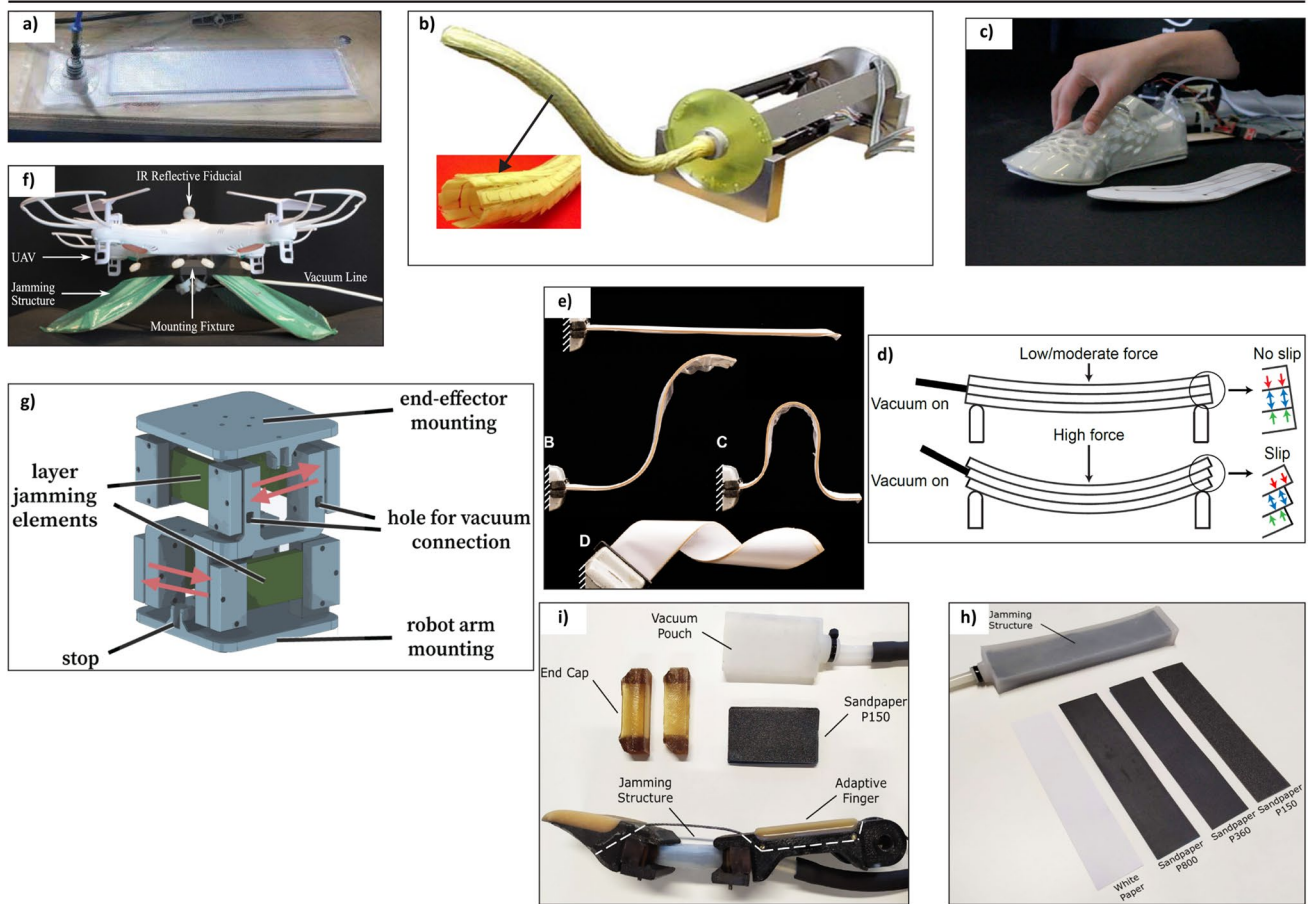


dielectric elastomer foils for controlling stiffness as shown in Fig. 11c [107]. Area moment of inertia of this beam was controlled via a proposed mechanism consisting of teeth structure and a stiffness ratio of 5.6 was achieved by them.

The principle of laminar jamming has also been explored for developing wearable robots to improve rehabilitation practices. As shown in Fig. 12a researchers developed VSU (variable stiffness unit) made of flexible textile layers (polyethylene terephthalate fiber) coated with PVC (polyvinyl chloride) film to increase static friction [108]. For the application of minimally invasive surgeries, researchers developed a scale type of laminar structure resembling the body of a snake as shown in Fig. 12b. A maximum resisting force of 2 N was achieved with the application of 101 kPa of pressure [109]. Inspired by the use of laminar jamming in soft robotics some researchers developed variable stiffness deformable day-to-day objects like furniture, shoes,

etc. [110]. Figure 12c shows a shoe whose stiffness can be controlled through laminar jamming [110]. In the research, 32 different types of thin sheet materials were surveyed including leather, sandpaper, Tyvek, copy paper, etc. [110]. Some researchers extensively experimented with laminar jamming with layers of printer copy paper as shown in Fig. 12e [21]. Analytical solutions of beam stiffness, strain energy, and deflection for pre-slip, transition, and full-slip regimes as presented in Fig. 12d [21]. Some researchers also reported the dynamic response of laminar jamming structures [111]. Figure 12f shows a quadcopter equipped with a laminar structure whose dynamic response helps minimize the landing force impact on the quadcopter [111]. Some researchers developed two degrees of freedom robotic wrist driven by a layer jamming mechanism as shown in Fig. 12g [112]. The proposed prototype demonstrated a large variation in stiffness (sixty-three times), sufficient for most

### Controlled stiffness using homogeneous laminar jamming



**Fig. 12** Homogeneous laminar jamming structures: (a) a laminar structure made from polyethylene terephthalate fiber layers coated with PVC [108]; (b) a laminar structure with scales constructed for minimally invasive surgeries [109]; (c) a shoe whose stiffness can be controlled via laminar jamming [110]; (d) no-slip and slip condition of the laminar structure [21]; (e) stability of laminar struc-

ture at increased vacuum pressure [21]; (f) quadcopter with laminar legs to control the dynamic shock response during landing [111]; (g) 2 degrees of freedom robotic wrist integrated with laminar jamming [112]; (h) laminar structure with layers of sandpaper [20]; (i) robotic finger integrated with sandpaper-based laminar structure at its joint [20]

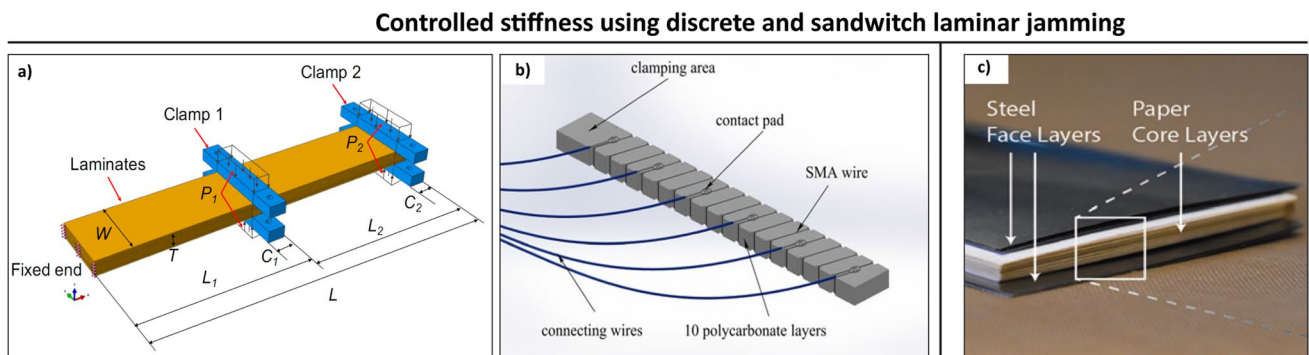
robotic applications [112]. The use of sandpapers for laminar jamming is also explored by some researchers [20]. P800, P360, and P150 size sandpapers were used to develop variable stiffness flexure joints for a robotic gripper as shown in Fig. 12h [20], the best results were offered by the jammer made from P150 size sandpaper. Figure 12i displays an adaptive finger developed with a jamming structure at its joint [20].

Some researchers investigated the discrete control of stiffness of laminar jammers by clamping a certain portion of layered material made from ABS (acrylonitrile butadiene styrene) as shown in Fig. 13a [113]. It was observed that clamping 10% of the beam area with only two clamps increases the bending stiffness approximately 17 times [113]. Some researchers also developed a multiple-layer polycarbonate jamming structure as shown in Fig. 13b [114], whose stiffness is discretely controlled via SMA wire wrapped

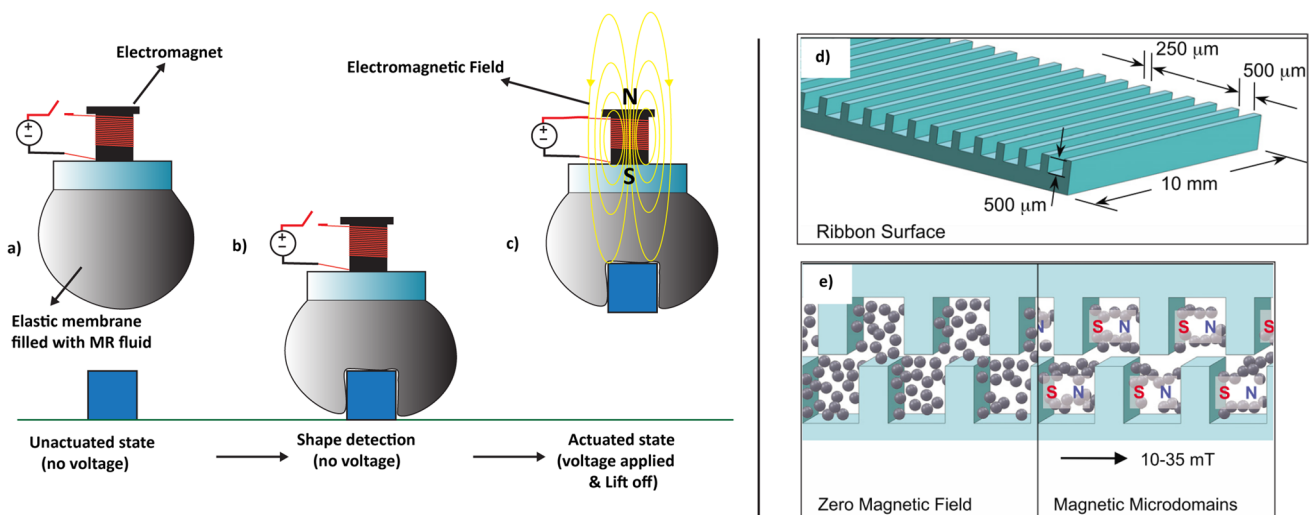
around its structure, and section-wise control of the beam was achieved [114]. Very recently some researchers are exploring laminar jamming composite structures investigating a tunable stiffness mechanism called ‘Sandwich jamming structure’ [22]. A composite structure was constructed by a group of researchers with laminar layers made of paper, PU (polyurethane), LDPE (low-density polyethylene), and low carbon steel as shown in Fig. 13c [22]. The reports concluded that an increase in stiffness to mass ratio was 1800 times compared to 550 times that of a jamming structure without composite layers [22].

### 3.8 Controlled stiffness through MR jamming

Figure 14a-c displays the operation of the MR fluid jammer. Figure 14a displays the unactuated state of the jammer, i.e., when no voltage is applied to the electromagnet, the



**Fig. 13** Discrete and sandwiched laminar jamming structures: (a) discrete control of laminar jamming structure using clamps [113]; (b) discrete control of laminar jamming structure using shape memory alloys [114]; (c) sandwiched laminar jamming structure [22]



**Fig. 14** Structure and operation of MR jammers: (a) MR jammer in unactuated state, no voltage applied; (b) shape detection by MR jammer; (c) stiffening of MR fluid and gripping of an object due to

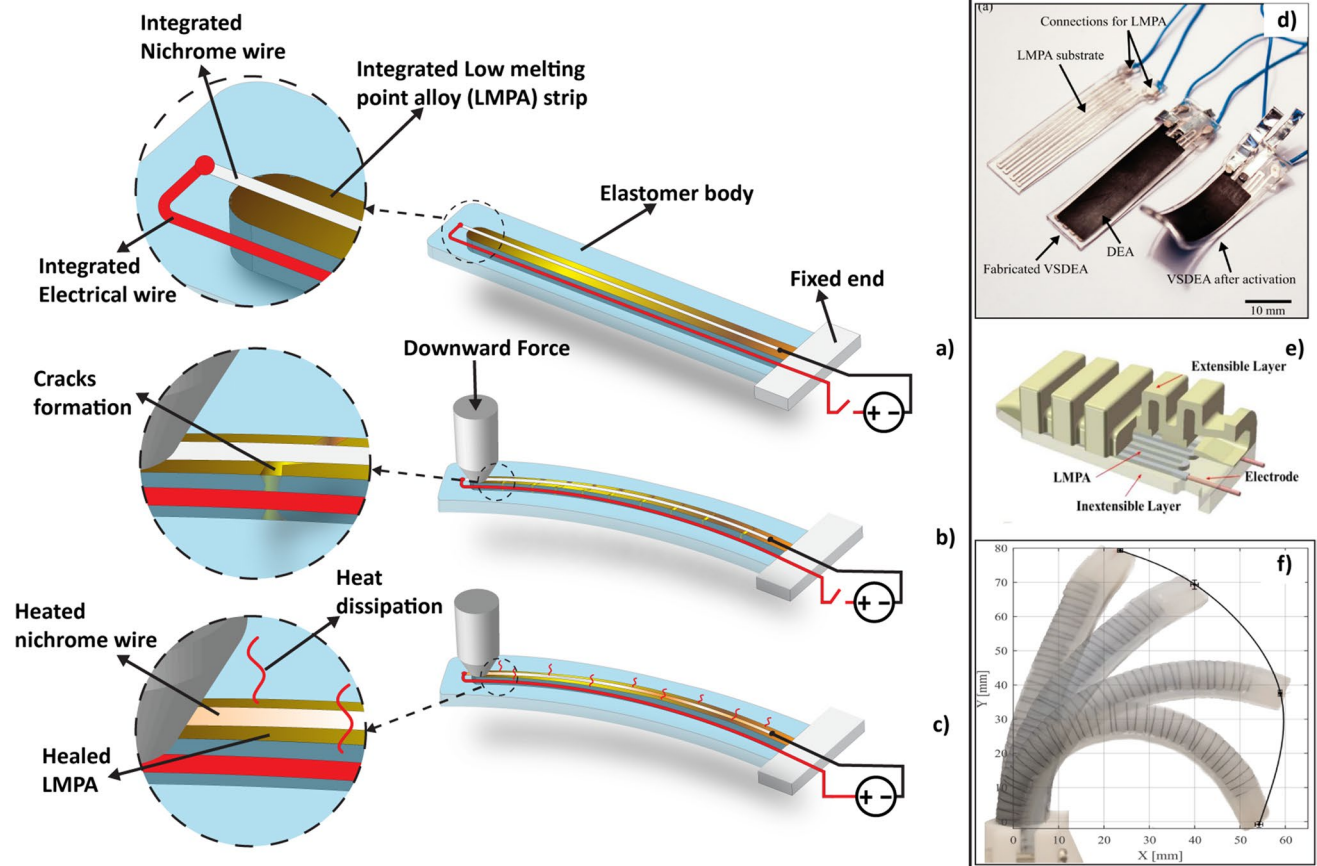
the magnetic field generated by the activated electromagnet; (d) micropatterned comb structure [23]; (e) interlocking state between two patterns due to magnetic field [23]

magnetic fluid is free to flow inside the membrane structure. Figure 14b displays the shape adjustment state where the jammer is still not activated. Figure 14c shows the actuation state of MR fluid which turns solid due to interaction with the magnetic field generated by the electromagnet. This rigidity of MR fluid is responsible for a good grip on an object which can be lifted and transported if the magnetic field exists. Apart from using MR fluid in this configuration, researchers have also developed layer jamming structures filled with MR fluid. Figure 14d [23] displays a micropatterned comb structure of 250  $\mu\text{m}$  in width. Two such surfaces exhibit a locking behavior when MR fluid-filled between them is exposed to 10 to 35 mT of the magnetic field as shown in Fig. 14e [23]. Such configuration is very useful to enhance the stiffness of low-powered portable soft robots.

### 3.9 Controlled stiffness through LMPA

Low melting point alloys (LMPAs) can be employed to develop soft robots with increased stiffness and self-healing

properties. LMPA consists of around 23% lead, 5% cadmium, 45% bismuth, 8% tin and 19% indium [24]. During the actuation of the robot, LMPA can be heated to prevent any resistive stiffness and allow the actuator to bend or rotate freely. The solidification of LMPA when cooled down at the specified position of the actuator causes an increase in stiffness. Figure 13 displays the principle of self-healing of LMPA based actuators. Figure 15a displays a soft actuator integrated with a strip of LMPA. The thickness of the LMPA strip depends on the stiffness [62] and the response time required by the actuator. The soft actuator is integrated with nichrome wire to supply heat to the LMPA strip. Such actuators are also integrated with flexible electrical wiring as shown in Fig. 15a to make an electrical connection to nichrome wire. In this configuration, the LMPA strip is in a cold solid-state as no electrical connections of nichrome wire are made to the external power source. When a downward force is applied at one end of the actuator as shown in Fig. 15b, cracks are formed throughout the LMPA strip. In this case, the LMPA strip tries to resist this force but



**Fig. 15** Structure and operation of LMPA actuators: (a) a soft actuator integrated with LMPA strip and nichrome wire in an un-actuated state; (b) formation of cracks in LMPA strip due to bending; (c) melting and healing of LMPA strip when integrated nichrome wire

is heated; (d) DEEA actuator integrated with LMPA [62]; (e) pneumatic actuator integrated with LMPA [24]; (f) silicone actuator filled with LMPA [63]

when the force exceeds the designed stiffness, cracks are formed and LMPA fails. However, this LMPA strip can be heated again as shown in Fig. 15c by connecting nichrome wire to an external power source. In this case, the LMPA strip achieves a molten state, due to heat generated from nichrome wire these cracks are healed. Figure 15d displays an actuator developed by some researchers composed of DEA and LMPA [62]. The proposed actuator used DEA for actuation and LMPA to provide stiffness. The studies reported that LMPA based actuator takes 30 s to melt at 1 Watt of power input and 60 s to cool and solidify [62]. It may be observed that the response time can be improved through the efficient design of the actuator with increased convection between LMPA and surroundings. Figure 15e shows a Pneunet actuator developed by some researchers [24]. The proposed actuator is integrated with LMPA and heated via an electrode. It was reported that a current of 4 A was required to melt LMPA from 26<sup>o</sup> to 48<sup>o</sup>C in 160 s and at 8 A the time was reduced to 37 s [24]. Figure 15f displays a silicone actuator developed by researchers filled with molten LMPA via a syringe pump [63]. In the unique configuration, LMPA provides both actuation and stiffness, and nichrome wire wrapped around the actuator heats LMPA [63]. It was reported that the LMPA actuator takes 300 s to solidify and 190 s to heat and convert into a molten form [63]. It can be observed that the large time delay required by LMPA to change its state is an added disadvantage that needs to be improved.

### 3.10 Comparison of soft actuators based on controlled stiffness

From Table 2, the input energy to actuate variable stiffness actuators can be in the form of vacuum pressure or application of low voltages as per published research. In the category of vacuum as an energy source, it can be observed that spherical granular jammers can exert high forces compared to actuators like linear granular jammers, and laminar jammers. The high force can be attributed to the spherical shape of a granular jammer in which the compressive force is applied from all directions to the object, while in linear granular jammers the quantity of granular material is linearly distributed along the longitudinal direction, due to which the compressive force is uniformly distributed along the axis. Similar is the case with laminar jammers. However, sandwiched laminar jammers can exert high forces up to 20 N [22] due to the presence of composite layers that can generate strong frictional forces under vacuum pressure. It may also be noted that the wet surface condition [72] of granular jammers increases the holding force generated by them, and it may be attributed to the property of such wet surfaces to create a temporary vacuum between two surfaces that holds the object even stronger.

Figure 16 depicts the range of forces generated by jamming actuators. It may be observed that in the category of low voltages as an energy source, MR jammers which are somewhat similar to the operation of granular jammers can exert high force up to 60 N [115]. LMPA jammers can exert forces up to 3 N [24], while actuators integrated with SMA can exert forces greater than 4 N [114]. It may be noted that structures integrated with LMPA or SMA exert comparable forces which may be attributed to the similarity in the principle of operation. In both actuators metal wires or strips are used to provide stiffness to the actuators which result in similar forces. The resistive force of such actuators can be further improved by increasing the amount of this integration, but it will increase the input energy requirement and increase its heat dissipation. Note that the values in Table 2 do not represent the ultimate performance of stiffness actuators and only provide quantified means for the comparison of such actuators.

Figure 17 compares pneumatic actuators and jammers in terms of the input pressure required. It may be concluded that McKibben and pneunet actuators generally require high pressures as compared to spherical jamming structures, also the vacuum pressure required by linear granular and laminar jamming structures is not much as the layers or grains are tightly packed and a small vacuum is sufficient to initialize the jamming state.

### 3.11 Advantages and disadvantages of soft actuators based on controlled stiffness

Granular jamming and laminar jamming structures are easy to construct and may be developed using inexpensive materials. The advantage of using granular jammers is their capability to grasp a variety of objects with complex shapes. Laminar jammers can be integrated with pneunets to increase the bending stiffness without influencing the overall functionality and volume of the actuator. The advantage of using LMPA jammers is their self-healing property. As per reports, more investigations in sandwiched laminar jamming structures may further improve its performance.

Granular jamming structures are bulky. As per reports, the use of abrasive material like sandpaper for fabricating the layers of the jamming structure decreases the actuator performance with time due to the wearing of abrasive surfaces. Therefore, the layer material of laminar jamming structures requires further investigations for sustainable performance. The self-healing of LMPA jammers requires appreciable time and is a slow process.

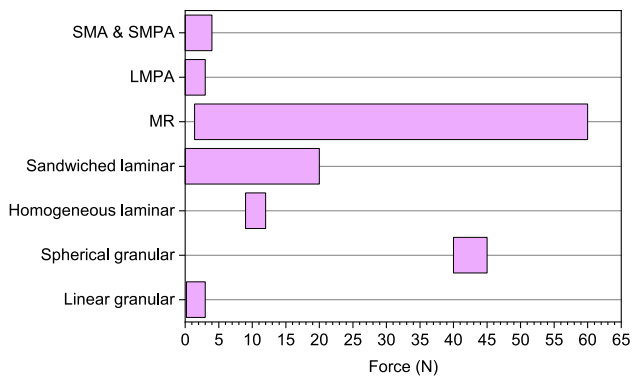
## 4 Controlled adhesion

Controlled adhesion is achieved using two main technologies, electroadhesion [29, 117, 118] and geckoadhesion [12, 119]. Electroadhesion is achieved through the applied

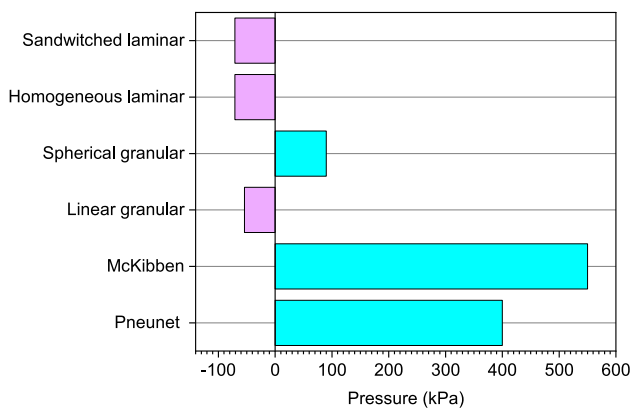
**Table 2** Comparison of the performance parameters of various soft actuators governed through controlled stiffness

| Energy source | Actuator Type                    | Area (mm <sup>2</sup> )/<br>Volume(mm <sup>3</sup> )/Dia<br>(mm)/Length of actuator<br>(mm)                 | Deflection(mm)                          | Test type   | Supplied Power<br>/Pressure/<br>Voltage/<br>Current   | Bending<br>stiffness(N/mm)/<br>Resistive force (N) | Infill material  | Surface Condition<br>(Wet/Dry) |
|---------------|----------------------------------|---|---|---|---|--|--|--------------------------------|
| Vacuum        | Linear granular<br>jammers       | 40 to 85 mm [80, 95,<br>104]  | 9 to 20 [80, 95,<br>104]                | Cantilever beam<br>test   | -10 to -54 kPa [80,<br>95, 104]   | 0.19 to 3 N [80, 95,<br>104]                       | Sugar [104], 6 mm<br>plastic spheres<br>[95], Polythene<br>filled with 4 mm<br>glass spheres [80]                              | dry [80, 95, 104]              |
|               | Spherical granular<br>jammers    | ~25 mm(object<br>size) [72],<br>50×11.5mm <sup>2</sup> (DxL)<br>[65]  | ~3.5 mm [72]                            | Compressive test<br>[65, 72]  | -80 to -89.9 kPa<br>[65, 72]  | 40 to 45 N [65, 72]                                | Rubber bag filled<br>with 100 µm glass<br>spheres [72], cof-<br>fee powder [65]  | Wet [72], dry [65]             |
|               | Homogeneous lami-<br>nar jammers | 250×50mm <sup>2</sup> (LxW)<br>[21],<br>50×27.5mm <sup>2</sup> (LxW)<br>[112]                               | 4 to 8 mm [21, 112]                     | Cantilever beam<br>test [21], 3-point<br>flexural test [112]  | -70 to -71 kPa [21,<br>112]   | 9 to 12 N [21, 112]                                | 20 to 100 layers of<br>printer paper [21,<br>112]  | dry [21, 112]                  |
|               | Sandwiched laminar<br>jammers    | 100×50mm <sup>2</sup> (LxW) [22]  | ~5 mm [22]                              | 3-point flexural test<br>[22]   | -71 kPa [22]  | > 20 N [22]  | 35 layers of paper<br>and steel sand-<br>wiched structure<br>[22]  | dry [22]                       |
| Low voltage   | MR jammers                       | 44,45 mm(D) cylin-<br>drical object [115],<br>25 mm(D) of gripper<br>[116]                                  | 4 to 8 mm [115,<br>116]                 | Compressive test<br>[115, 116]  | 3A [115], 3.5 W<br>[116]  | 1.4 to 60 N [115,<br>116]                          | MR fluid [115, 116]  | dry [115, 116]                 |
|               | LMPA jammers                     | 40×10x1mm <sup>3</sup> (LxWxT)<br>[62],<br>1.4×1.4mm <sup>2</sup> (LMPA<br>section<br>size), 100 mm(L) [63] | Negligible [62], 7<br>to 14 mm [24, 63] | Cantilever beam<br>test [24, 62],<br>Aligned vertically<br>and force applied<br>horizontally on<br>tip [63] | 3 kV [62], 4<br>to ~8A(to melt<br>LMPA) [24],<br>DC supply with<br>PID temperature<br>controller [63] | 2mN [62], 2 to 3 N<br>[24, 63]                     | DEA integrated<br>with LMPA<br>[62], Pneumet<br>integrated with<br>LMPA [24],<br>Silicone actuator<br>filled with LMPA<br>[63] | dry [24, 62, 63]               |
|               | SMA & SMPA<br>jammers            | 7.5 mm thick laminar<br>jammer [114]  | > 2 mm [114]                            | Cantilever beam<br>test [114]   | 0.5A [114]  | > 4 N [114]  | Polycarbonate<br>layers spirally<br>winded with<br>0.2 mm dia shape<br>memory alloy<br>wire [114]                              | dry [114]                      |





**Fig. 16** Comparison of range of bending and compressive forces generated by jamming actuators



**Fig. 17** Comparison of the input range of pressure required by pneumatic actuators and jamming structures

electric field (require few kV) which creates an electrostatic attraction between two surfaces, while gecko adhesion is typically inspired by nature, the grippers that are designed using geckoadhesion utilize the strong van der Waals forces which are acting between the designed microstructures and object surface.

#### 4.1 Controlled adhesion through electroadhesion

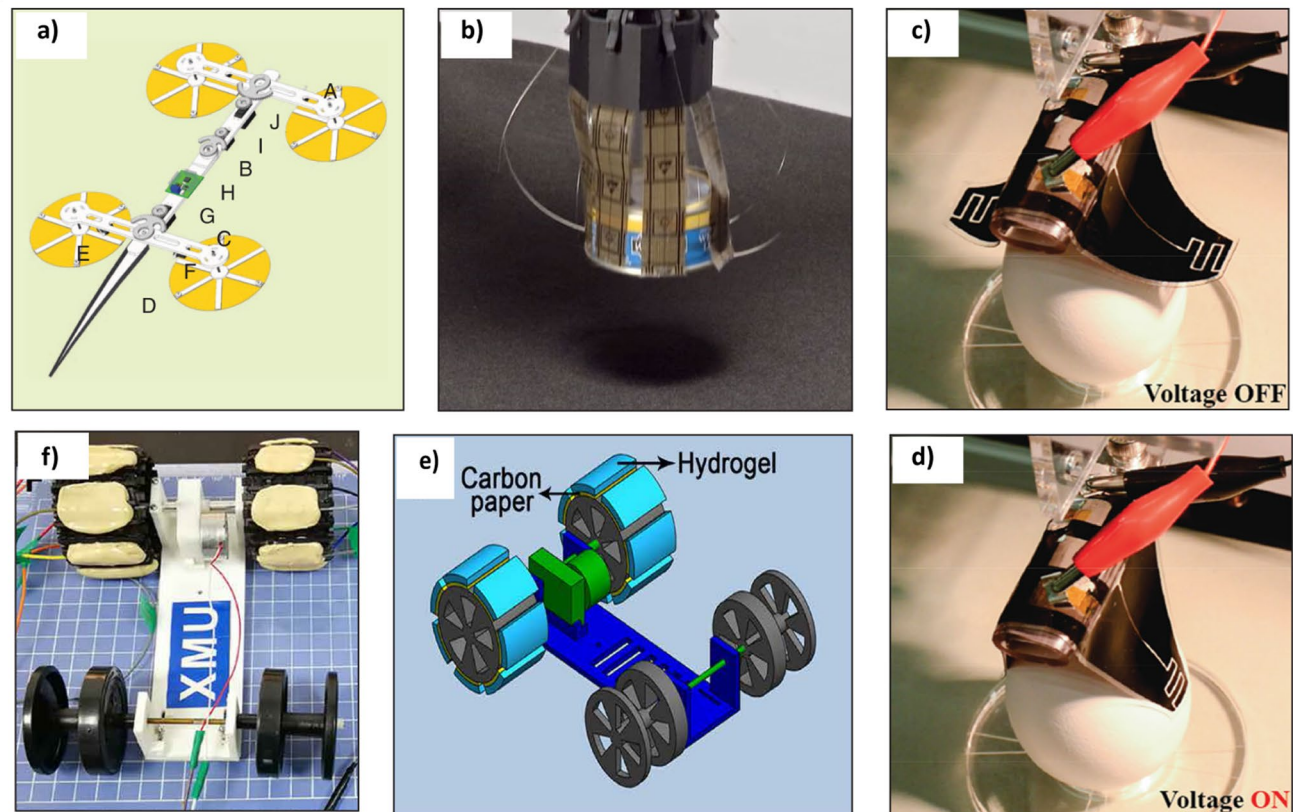
To effectively utilize the electroadhesion it is essential to widen electric fields for maximum electrostatic attraction or repulsion, for this, the electrodes are designed in an interdigitated fashion such as spiral shapes that can create out of plane electric fields. Optimizing the electrode geometry (such as gap & width) and thickness of insulation material improves the overall performance of electroadhesion based grippers [29, 117, 118]. Electroadhesive grippers can be used for sensitive jobs like handling silicon wafers [120] and climbing walls [121].

Figure 18a displays the computer-aided design of a gecko-inspired electroadhesive robot [121], the mechanism of which is actuated via servo motors. Researchers estimated that with 3 kV of the input voltage the adhesive footpads can produce 3.2 N of force on the glass. In soft robotic grippers, electroadhesion may be combined with actuation systems driven by electromagnetic motors, such type of gripper was used by Grabit company in the past to pick a variety of objects [122], it can be observed from Fig. 18b this gripper is made of flexible PCB with interdigitated electrodes. Some researchers also combined electroadhesion with dielectric (DE) actuation to form a compact sleek gripper [123]. With the novel arrangement of electrodes in this gripper, both the in membrane electric fields and fringing electric fields are maximized generating over 10 times higher electroadhesion force [123] compared to any conventional dielectric actuation system. Figure 18c displays this gripper under-voltage off conditions. Figure 18d displays the same gripper when 3.5 kV is applied to pick an egg weighing 60.9 g. In general, electroadhesive grippers are lightweight but require high voltages to actuate. Also, the problem of small hysteresis after turning off the voltage is prominent which reduces the response time of such grippers, the residual force due to hysteresis can last a few seconds for dielectric objects [124]. Some electroadhesive hydrogels [30] were also developed by researchers which can be activated using low voltages like 3.0 to 4.5 V, Fig. 18e displays the computer-aided design of a wheeled robot equipped with such hydrogel [30]. Figure 18f displays the actual prototype of a wall-climbing robot equipped with TBVA electroadhesive hydrogels at its wheels.

#### 4.2 Controlled adhesion through geckoadhesion

Researchers have developed biologically inspired microfibers [10, 125, 126] similar to the natural fibers gifted by mother nature which helpsome creatures climb walls effectively. When such microfibers are pressed against the object's surface in the normal direction, geckoadhesion is activated, and removing this pressure on the surface deactivates this adhesion. Wall climbing robots [28] and human climbing [127] systems have been developed using this adhesion technology. Figure 19a displays the SEM micrography of a 6  $\mu\text{m}$  diameter SU-8 polymer developed by researchers using lithography, such structure bears the properties of geckoadhesion [126]. Another group of researchers developed a robot named 'Stikybot' as shown in Fig. 19b [28]. It is designed with directional polymer stacks (DPS) on its feet, it can walk with a speed of 4 cm/s on the vertical tile surface and 24 cm/s on horizontal surfaces. Some researchers inspired by the "Tokay gecko" developed a PDMS micro wedge adhesive (100  $\mu\text{m}$  tall) following roughly the power-law  $\sigma_{\text{max}} \propto A^{-1/50}$  [127]. As shown in Fig. 19c using this

## Controlled adhesion using electroadhesion



**Fig. 18** Controlled adhesion using electroadhesion: (a) gecko-inspired electroadhesive robot [121]; (b) electroadhesive gripper with flexible PCB fingers developed by Grabit inc [122]; (c) voltage off condition of DE actuator integrated with electroadhesive strips [123];

(d) voltage on condition of DE actuator integrated with electroactive strips [123]; (e) computer-aided design of the hydrogel-based wall-climbing robot [30]; (f) actual prototype of the wall-climbing robot with hydrogel on its wheels [30]

system a human weighing 70 kg was able to ascend a height of 3.7 m on a vertical glass wall using 140 cm<sup>2</sup> of developed adhesive in each hand.

### 4.3 Comparison of soft actuators based on controlled adhesion

From Table 3 the reports suggest that a gecko adhesive actuator can be used to lift a person weighing 70 kg when the surface area of the adhesive is appropriately chosen [127]. The adhesive force of a gecko adhesive is proportional to its surface area, which may be attributed to the fact that as the surface area of adhesive increases the number of microfibers increases.

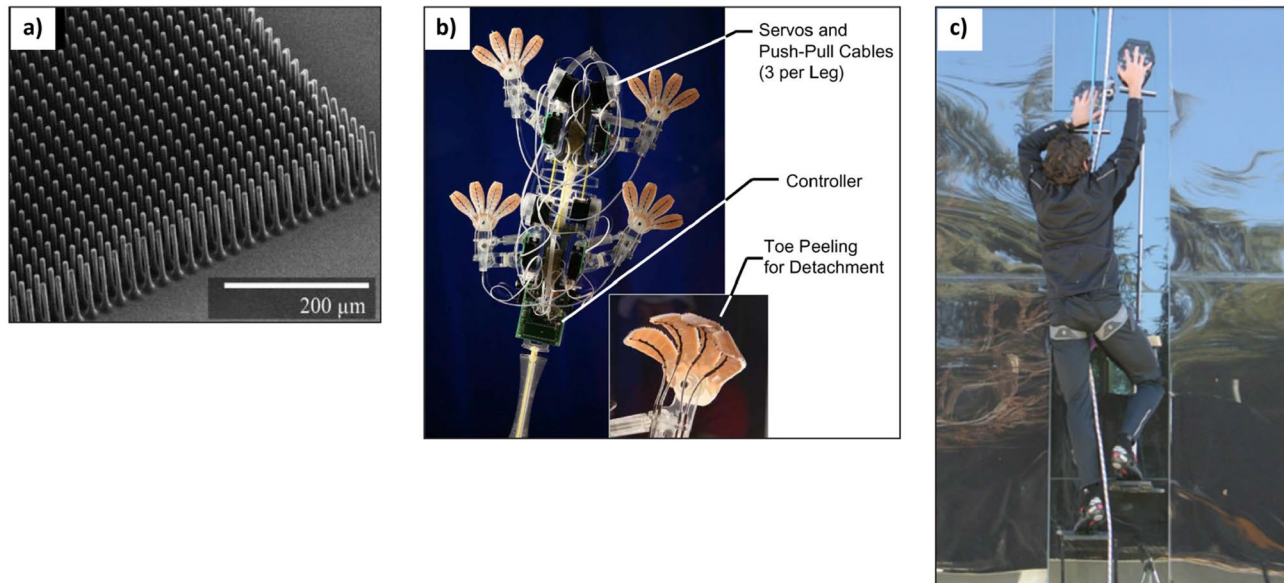
Adhesive actuators whether gecko adhesive, electrostatic, or hydrogel in nature are effective on vertical surfaces, and the effectiveness of adhesion also depends on the surface properties. Geckoadhesives and electrostatic

actuators are mostly effective on glass surfaces [28, 121, 127] as the smooth surface of glass allows more contact between its surface and the surface of micropillars of a gecko adhesive. Also, the low voltage-driven hydrogel is effective on stainless steel surfaces [30] as it requires a conductive surface for adhesion. Note that Table 3 does not present the ultimate performance of adhesive actuators and only provides some quantified means for the comparison of these actuators.

### 4.4 Advantages and disadvantages of soft actuators based on controlled adhesion

Gecko adhesive actuators require no external energy source like electric power or pneumatic pressure but only the normal force. As per reports geckoadhesives can be manufactured easily using molding of soft silicone materials. Electroadhesive actuators are light in weight with a high load-to-weight ratio.

## Controlled adhesion using geckoadhesion



**Fig. 19** Controlled adhesion using geckoadhesion: (a) SEM micrograph of 6  $\mu\text{m}$  diameter SU-8 polymer gecko adhesive [126]; (b) stickybot robot with DPS on its feet [28]; (c) human climbing device made using PDMS micro wedge adhesive technology [127]

The low voltage electroadhesive hydrogels can be molded like clay into any desired shape based on the application.

However, electroadhesive actuators require high voltages in the range of kilovolts to operate, which require high voltage power supplies. Safe electrical isolation of electroadhesives is necessary and requires additional attention. Also, more investigations are required in material science to enhance the Geckoadhesive technology for practical usage.

### 5 Prospective and future challenges

This study revealed that Mckibben actuators can generate high forces compared to pneumatic actuators, but they also require high-pressure air. Future studies can investigate improving the portability and energy consumption of mckibben and pneumatic actuators. Further studies can focus on increasing the force exerted by dielectric and ionic polymer metal composite actuators through composite interface materials. The electrical isolation of dielectric actuators needs to be explored for their safe application in the assistance of surgeries and consumer robotics. Future investigations can focus on novel mechanisms to apply discrete pressure on laminar jamming structures. Investigations on the use of smart materials like SMA and SMPA in laminar jamming will help reduce the dependency on vacuum energy and make laminar jammers energy efficient and applicable to

mobile robotics. Further investigations on composite materials with enhanced friction properties and flexibility will help improve the stiffness of laminar jammers. Investigations on the effect of temperature on frictional properties of laminar jammer need to be explored. Cost-effective geckoadhesives need to be investigated. New materials need to be explored which can be micro molded to fabricate strong geckoadhesives with high adhesive force to adhesion area ratio.

### 6 Summary and concluding remarks

The applications of soft robotics are diverse and range from space exploration to performing minimally invasive surgeries to lifting soft vegetables. However, they require controlling techniques to tune their rigidity or enhance their adhesion properties. Based on the recent reports, this article provides a detailed explanation of the controlling technologies that can be utilized to enhance the functionalities of a soft robot. After a thorough analysis of the techniques to control the actuation, it was revealed that recently developed Peano HASEL actuators due to their high resistive force can be used to develop next-generation artificial muscles. Investigations on the possible stiffening techniques revealed that MR jammers have high load carrying capacity, but in terms of high stiffness to volume ratio, sandwiched laminar jammers provide a promising future to develop low-cost,

**Table 3** Comparison of the performance parameters of various soft actuators governed through controlled adhesion

| Energy source | Actuator Type           | Area(mm <sup>2</sup> )/<br>Volume(mm <sup>3</sup> )/<br>Dia(mm)/Length of actuator/<br>system(mm)                                  | Supplied Power<br>/Pressure/<br>Voltage/<br>Current                           | Holding force/<br>weight          | Angle of inclination | Surface of attraction      | Adhesive material  |
|---------------|-------------------------|--|---|-----------------------------------|----------------------|----------------------------|--|
| Normal force  | Gecko adhesive actuator | 600×200×60mm <sup>3</sup> (L×W×H)<br>robot size [28], 140cm <sup>2</sup><br>adhesive tile in each hand<br>[127]                    | ~ 2.5 N (Tangential force)<br>[28], Compressive force<br>by human hands [127] | 370 g [28], 70 kg<br>person [127] | Vertical [28, 127]   | Glass surface [28,<br>127] | Soft polyurethane<br>[28], PDMS micro<br>wedge adhesive<br>[127] |
| High voltage  | Electrostatic actuator  | 170 mm(D) [121]  | 3000 V [121]  | 3.2 N [121]                       | Vertical [121]       | Glass surface [121]        | Polyimide film with<br>interdigital copper<br>electrodes [121]   |
| Low voltage   | Hydrogel actuator       | Foot A of robot:<br>60 × 18 × 4 mm <sup>3</sup> (L × W × H)<br>Foot B of robot:<br>75 × 27 × 4 mm <sup>3</sup> (L × W × H)<br>[30] | -3 to 3 V DC [30]   | 113 g [30]                        | 85° [30]             | Stainless Steel [30]       | TBVA hydrogel [30]   |

portable, and energy-efficient hybrid soft robots with tunable stiffness. However, future investigations on the development of laminar jammers made of advanced composite materials are required. Investigations are required on self-healing actuators based on LMPA to reduce their response time by improving their thermal properties. More investigations on improving the electric isolation properties of electroadhesives are required for safe use in micro-robotics and consumer soft robots.

**Author Contributions** **Kunal Singh:** Conceptualization, Investigation, Formal analysis, Visualization, Writing—original draft, Writing – review editing; **Shilpa Gupta:** Conceptualization, Formal analysis, Writing – original draft, Writing – review editing, Supervision.

**Code Availability** Not applicable.

**Declarations**

**Conflict of Interest** The authors declare no conflict of interest.

**Ethics Approval** Not applicable.

**Consent to Participate** Not applicable.

**Consent for Publication** Not applicable.

**References**

1. Kim, S., Laschi, C., Trimmer, B.: Soft robotics: a bioinspired evolution in robotics. *Trends Biotechnol.* **31**, 287–294 (2013). <https://doi.org/10.1016/j.tibtech.2013.03.002>
2. Nakajima, K., Hauser, H., Li, T., Pfeifer, R.: Information processing via physical soft body. *Sci. Rep.* **5**, 1–11 (2015). <https://doi.org/10.1038/srep10487>
3. Zhang, S., Ke, X., Jiang, Q., Ding, H., Wu, Z.: Programmable and reprocessable multifunctional elastomeric sheets for soft origami robots. *Sci. Robot.* **6**, 1–13 (2021). <https://doi.org/10.1126/scirobotics.abd6107>
4. Liu, Q., Gu, X., Tan, N., Ren, H.: Soft Robotic Gripper Driven by Flexible Shafts for Simultaneous Grasping and In-Hand Cap Manipulation. *IEEE Trans. Autom. Sci. Eng.* **18**, 1134–1143 (2021). <https://doi.org/10.1109/TASE.2020.2997076>
5. Henke, M., Sorber, J., Gerlach, G.: EAP-Actuators with Improved Actuation Capabilities for Construction Elements with Controllable Stiffness. *Adv. Sci. Technol.* **79**, 75–80 (2012). <https://doi.org/10.4028/www.scientific.net/ast.79.75>
6. Li, C., Lau, G.C., Yuan, H., Aggarwal, A., Dominguez, V.L., Liu, S., Sai, H., Palmer, L.C., Sather, N.A., Pearson, T.J., Freedman, D.E., Amiri, P.K., de la Cruz, M.O., Stupp, S.I.: Fast and programmable locomotion of hydrogel-metal hybrids under light and magnetic fields. *Sci. Robot.* **5**, (2020). <https://doi.org/10.1126/scirobotics.abb9822>
7. Shintake, J., Cacucciolo, V., Floreano, D., Shea, H.: Soft Robotic Grippers. *Adv. Mater.* **30**, (2018). <https://doi.org/10.1002/adma.201707035>

8. Fitzgerald, S.G., Delaney, G.W., Howard, D.: A Review of Jamming Actuation in Soft Robotics. *Actuators*. **9**, 104 (2020). <https://doi.org/10.3390/act9040104>
9. Walker, J., Zidek, T., Harbel, C., Yoon, S., Strickland, F.S., Kumar, S., Shin, M.: Soft robotics: A review of recent developments of pneumatic soft actuators. *Actuators*. **9**, (2020). <https://doi.org/10.3390/act9010003>
10. Boesel, L.F., Cremer, C., Arzt, E., Campo, A.D.: Gecko-inspired surfaces: A path to strong and reversible dry adhesives. *Adv. Mater.* **22**, 2125–2137 (2010). <https://doi.org/10.1002/adma.200903200>
11. Wang, W., Ahn, S.: Shape Memory Alloy-Based Soft Gripper with Variable Stiffness for Compliant and Effective Grasping. *Soft Robot*. **4**, 379–389 (2017). <https://doi.org/10.1089/soro.2016.0081>
12. Cutkosky, M.R.: Climbing with adhesion: from bioinspiration to biounderstanding. *Interface Focus*. **5**, 20150015 (2015). <https://doi.org/10.1098/rsfs.2015.0015>
13. Kim, Y., Cha, Y.: Soft Pneumatic Gripper With a Tendon-Driven Soft Origami Pump. **8**, 1–11 (2020). <https://doi.org/10.3389/fbioe.2020.00461>
14. Mohd Ghazali, F.A., Mah, C.K., AbuZaiter, A., Chee, P.S., Mohamed Ali, M.S.: Soft dielectric elastomer actuator micro-pump. *Sensors Actuators A Phys.* **263**, 276–284 (2017). <https://doi.org/10.1016/j.sna.2017.06.018>
15. Kim, O., Kim, S.J., Park, M.J.: Low-voltage-driven soft actuators. *Chem. Commun.* **54**, 4895–4904 (2018). <https://doi.org/10.1039/C8CC01670D>
16. Zhao, S., Li, D., Xiang, J.: Design and application of PneuNets bending actuator. *Aircr. Eng. Aerosp. Technol.* **92**, 1539–1546 (2020). <https://doi.org/10.1108/AEAT-07-2019-0140>
17. Wakimoto, S., Suzumori, K., Kanda, T.: Development of intelligent McKibben actuator. In: 2005 IEEE/RSJ International Conference on Intelligent Robots and Systems. pp. 487–492. IEEE, Seoul, Korea (South) (2005)
18. Youn, J.H., Jeong, S.M., Hwang, G., Kim, H., Hyeon, K., Park, J., Kyung, K.U.: Dielectric elastomer actuator for soft robotics applications and challenges. *Appl. Sci.* **10**, (2020). <https://doi.org/10.3390/app10020640>
19. Mitchell, S.K., Wang, X., Acome, E., Martin, T., Ly, K., Kellaris, N., Venkata, V.G., Keplinger, C.: An Easy-to-Implement Toolkit to Create Versatile and High-Performance HASEL Actuators for Untethered Soft Robots. *Adv. Sci.* **6**, (2019). <https://doi.org/10.1002/advs.201900178>
20. Gerez, L., Gao, G., Liarokapis, M.: Laminar Jamming Flexure Joints for the Development of Variable Stiffness Robot Grippers and Hands. In: 2020 IEEE/RSJ International Conference on Intelligent Robots and Systems (IROS). pp. 8709–8715. IEEE, Las Vegas, NV, USA (2020)
21. Narang, Y.S., Vlassak, J.J., Howe, R.D.: Mechanically Versatile Soft Machines through Laminar Jamming. *Adv. Funct. Mater.* **28**, 1707136 (2018). <https://doi.org/10.1002/adfm.201707136>
22. Narang, Y.S., Aktaş, B., Ornellas, S., Vlassak, J.J., Howe, R.D.: Lightweight Highly Tunable Jamming-Based Composites. *Soft Robot*. **7**, 724–735 (2020). <https://doi.org/10.1089/soro.2019.0053>
23. Majidi, C., Wood, R.J.: Tunable elastic stiffness with microconfined magnetorheological domains at low magnetic field. *Appl. Phys. Lett.* **97**, 2012–2015 (2010). <https://doi.org/10.1063/1.3503969>
24. Yufei, H., Tianmiao, W., Xi, F., Kang, Y., Ling, M., Juan, G., Li, W.: A variable stiffness soft robotic gripper with low-melting-point alloy. In: 2017 36th Chinese Control Conference (CCC). pp. 6781–6786. IEEE, Dalian, China (2017)
25. Liao, T., Kalairaj, M.S., Cai, C.J., Tse, Z.T.H., Ren, H.: Fully-Printable Soft Actuator with Variable Stiffness by Phase Transition and Hydraulic Regulations. *Actuators*. **10**, 269 (2021). <https://doi.org/10.3390/act10100269>
26. Hoang, T.T., Quek, J.J.S., Thai, M.T., Phan, P.T., Lovell, N.H., Do, T.N.: Soft robotic fabric gripper with gecko adhesion and variable stiffness. *Sensors Actuators, A Phys.* **323**, 112673 (2021). <https://doi.org/10.1016/j.sna.2021.112673>
27. Germann, J., Schubert, B., Floreano, D.: Stretchable electroadhesion for soft robots. In: IEEE International Conference on Intelligent Robots and Systems. pp. 3933–3938. IEEE, Chicago, IL, USA (2014)
28. Smooth Vertical Surface Climbing With Directional Adhesion: Sangbae Kim, Spenko, M., Trujillo, S., Heyneman, B., Santos, D., Cutkosky, M.R. *IEEE Trans. Robot.* **24**, 65–74 (2008). <https://doi.org/10.1109/TRO.2007.909786>
29. Liu, R., Chen, R., Shen, H., Zhang, R.: Wall Climbing Robot Using Electrostatic Adhesion Force Generated by Flexible Interdigital Electrodes. *Int. J. Adv. Robot. Syst.* **10**, 36 (2013). <https://doi.org/10.5772/54634>
30. Huang, J., Liu, Y., Yang, Y., Zhou, Z., Mao, J., Wu, T., Liu, J., Cai, Q., Peng, C., Xu, Y., Zeng, B., Luo, W., Chen, G., Yuan, C., Dai, L.: Electrically programmable adhesive hydrogels for climbing robots. *Sci. Robot.* **6**, eabl858 (2021). <https://doi.org/10.1126/scirobotics.abe1858>
31. Ni, X., Liao, C., Li, Y., Zhang, Z., Sun, M., Chai, H., Wu, H., Jiang, S.: Experimental study of multi-stable morphing structures actuated by pneumatic actuation. *Int. J. Adv. Manuf. Technol.* **108**, 1203–1216 (2020). <https://doi.org/10.1007/s00170-020-05301-1>
32. Christianson, C., Goldberg, N.N., Deheyn, D.D., Cai, S., Tolley, M.T.: Translucent soft robots driven by frameless fluid electrode dielectric elastomer actuators. *Sci. Robot.* **3**, eaat1893 (2018). <https://doi.org/10.1126/scirobotics.aat1893>
33. Rodrigue, H., Wang, W., Kim, D., Ahn, S.: Curved shape memory alloy-based soft actuators and application to soft gripper. *Compos. Struct.* **176**, 398–406 (2017). <https://doi.org/10.1016/j.compstruct.2017.05.056>
34. Mitchell, S.K., Wang, X., Acome, E., Martin, T., Ly, K., Kellaris, N., Venkata, V.G., Keplinger, C.: An Easy-to-Implement Toolkit to Create Versatile and High-Performance HASEL Actuators for Untethered Soft Robots. *Adv. Sci.* **1900178**, 1900178 (2019). <https://doi.org/10.1002/advs.201900178>
35. Wang, Z., Or, K., Hirai, S.: A dual-mode soft gripper for food packaging. *Rob. Auton. Syst.* **125**, 103427 (2020). <https://doi.org/10.1016/j.robot.2020.103427>
36. Joe, S., Totaro, M., Wang, H., Beccai, L.: Development of the Ultralight Hybrid Pneumatic Artificial Muscle: Modelling and optimization. *PLoS ONE* **16**, e0250325 (2021). <https://doi.org/10.1371/journal.pone.0250325>
37. Manns, M., Morales, J., Frohn, P.: Additive manufacturing of silicon based PneuNets as soft robotic actuators. *Procedia CIRP*. **72**, 328–333 (2018). <https://doi.org/10.1016/j.procir.2018.03.186>
38. Zhao, H., Li, Y., Elsamadisi, A., Shepherd, R.: Scalable manufacturing of high force wearable soft actuators. *Extrem. Mech. Lett.* **3**, 89–104 (2015). <https://doi.org/10.1016/j.eml.2015.02.006>
39. Shepherd, R.F., Ilievski, F., Choi, W., Morin, S.A., Stokes, A.A., Mazzeo, A.D., Chen, X., Wang, M., Whitesides, G.M.: Multi-gait soft robot. *Proc. Natl. Acad. Sci.* **108**, 20400–20403 (2011). <https://doi.org/10.1073/pnas.1116564108>
40. Drotman, D., Jadhav, S., Sharp, D., Chan, C., Tolley, M.T.: Electronics-free pneumatic circuits for controlling soft-legged robots. *Sci. Robot.* **6**, (2021). <https://doi.org/10.1126/SCIROBOTICS.AAY2627>

41. Stano, G., Arleo, L., Percoco, G.: Additive manufacturing for soft robotics: Design and fabrication of airtight, monolithic bending PneuNets with embedded air connectors. *Micromachines*. **11**, (2020). <https://doi.org/10.3390/M111050485>
42. Haghighashtiani, G., Habtour, E., Park, S.H., Gardea, F., McAlpine, M.C.: 3D printed electrically-driven soft actuators. *Extrem. Mech. Lett.* **21**, 1–8 (2018). <https://doi.org/10.1016/j.eml.2018.02.002>
43. Schlatter, S., Illenberger, P., Rosset, S.: Peta-pico-Voltron: An open-source high voltage power supply. *HardwareX*. **4**, e00039 (2018). <https://doi.org/10.1016/j.ohx.2018.e00039>
44. Ji, X., Liu, X., Cacucciolo, V., Imboden, M., Civet, Y., Haitami, A. El, Cantin, S., Perriard, Y., Shea, H.: An autonomous untethered fast soft robotic insect driven by low-voltage dielectric elastomer actuators. *Sci. Robot.* **4**, (2019). <https://doi.org/10.1126/scirobotics.aaz6451>
45. Lin, H.-T., Leisk, G.G., Trimmer, B.: GoQBot: a caterpillar-inspired soft-bodied rolling robot. *Bioinspir. Biomim.* **6**, 026007 (2011). <https://doi.org/10.1088/1748-3182/6/2/026007>
46. Lendlein, A.: Fabrication of reprogrammable shape-memory polymer actuators for robotics. *Sci. Robot.* **3**, eaat9090 (2018). <https://doi.org/10.1126/scirobotics.aat9090>
47. Seok, S., Onal, C.D., Cho, K.J., Wood, R.J., Rus, D., Kim, S.: Meshworm: A peristaltic soft robot with antagonistic nickel titanium coil actuators. *IEEE/ASME Trans. Mechatronics*. **18**, 1485–1497 (2013). <https://doi.org/10.1109/TMECH.2012.2204070>
48. Yoder, Z., Kellaris, N., Chase-Markopoulou, C., Ricken, D., Mitchell, S.K., Emmett, M.B., Weir, R.F. f., Segil, J., Keplinger, C.: Design of a High-Speed Prosthetic Finger Driven by Peano-HASEL Actuators. *Front. Robot. AI*. **7**, 181 (2020). <https://doi.org/10.3389/FROBT.2020.586216/BIBTEX>
49. Kothera, C.S., Jangid, M., Sirohi, J., Wereley, N.M.: Experimental Characterization and Static Modeling of McKibben Actuators. In: *Aerospace*. pp. 357–367. *ASMEDC* (2006)
50. Cacucciolo, V., Nabae, H., Suzumori, K., Shea, H.: Electrically-Driven Soft Fluidic Actuators Combining Stretchable Pumps With Thin McKibben Muscles. *Front. Robot. AI*. **6**, 146 (2020). <https://doi.org/10.3389/frobt.2019.00146>
51. Kurumaya, S., Nabae, H., Endo, G., Suzumori, K.: Design of thin McKibben muscle and multifilament structure. *Sensors Actuators A Phys.* **261**, 66–74 (2017). <https://doi.org/10.1016/J.SNA.2017.04.047>
52. Araromi, O.A., Burgess, S.C.: A finite element approach for modelling multilayer unimorph dielectric elastomer actuators with inhomogeneous layer geometry. *Smart Mater. Struct.* **21**, (2012). <https://doi.org/10.1088/0964-1726/21/3/032001>
53. Lau, G.-K., Goh, S.C.-K., Shiau, L.-L.: Dielectric elastomer unimorph using flexible electrodes of electrolessly deposited (ELD) silver. *Sensors Actuators A Phys.* **169**, 234–241 (2011). <https://doi.org/10.1016/j.sna.2011.04.037>
54. Goh, S.C.-K., Lau, G.-K.: Dielectric elastomeric bimorphs using electrolessly deposited silver electrodes. In: Bar-Cohen, Y. (ed.) *Electroactive Polymer Actuators and Devices (EAPAD) 2010*. p. 764215. *SPIE*, San Diego, California, United States (2010)
55. Franke, M., Ehrenhofer, A., Lahiri, S., Henke, E.F.M., Wallmersperger, T., Richter, A.: Dielectric Elastomer Actuator Driven Soft Robotic Structures With Bioinspired Skeletal and Muscular Reinforcement. *Front. Robot. AI*. **7**, 178 (2020). <https://doi.org/10.3389/FROBT.2020.510757/BIBTEX>
56. Rothmund, P., Kellaris, N., Mitchell, S.K., Acome, E., Keplinger, C.: HASEL Artificial Muscles for a New Generation of Lifelike Robots—Recent Progress and Future Opportunities. *Adv. Mater.* **33**, 1–28 (2021). <https://doi.org/10.1002/adma.202003375>
57. Liu, J., Xu, L., He, C., Lu, X., Wang, F.K.: Transparent low-voltage-driven soft actuators with silver nanowires Joule heaters. *Polym. Chem.* **12**, 5251–5256 (2021). <https://doi.org/10.1039/d1py00837d>
58. Shahinpoor, M.: Ionic polymer-conductor composites as biomimetic sensors, robotic actuators and artificial muscles - A review. *Electrochim. Acta.* **48**, 2343–2353 (2003). [https://doi.org/10.1016/S0013-4686\(03\)00224-X](https://doi.org/10.1016/S0013-4686(03)00224-X)
59. Shahinpoor, M.: Chapter 1. Fundamentals of Ionic Polymer Metal Composites (IPMCs). In: *RSC Smart Materials*. pp. 1–60. *Royal Society of Chemistry* (2015)
60. Wang, W., Yu, C.Y., Abrego Serrano, P.A., Ahn, S.H.: Shape Memory Alloy-Based Soft Finger with Changeable Bending Length Using Targeted Variable Stiffness. *Soft Robot.* **7**, 283–291 (2020). <https://doi.org/10.1089/soro.2018.0166>
61. Liu, M., Hao, L., Zhang, W., Zhao, Z.: A novel design of shape-memory alloy-based soft robotic gripper with variable stiffness. *Int. J. Adv. Robot. Syst.* **17**, 172988142090781 (2020). <https://doi.org/10.1177/1729881420907813>
62. Shintake, J., Schubert, B., Rosset, S., Shea, H., Floreano, D.: Variable stiffness actuator for soft robotics using dielectric elastomer and low-melting-point alloy. In: *2015 IEEE/RSJ International Conference on Intelligent Robots and Systems (IROS)*. pp. 1097–1102. *IEEE*, Hamburg, Germany (2015)
63. Peters, J., Nolan, E., Wiese, M., Miodownik, M., Spurgeon, S., Arezzo, A., Raatz, A., Wurdemann, H.A.: Actuation and stiffening in fluid-driven soft robots using low-melting-point material. In: *2019 IEEE/RSJ International Conference on Intelligent Robots and Systems (IROS)*. pp. 4692–4698. *IEEE*, Macau, China (2019)
64. Fujita, M., Ikeda, S., Fujimoto, T., Shimizu, T., Ikemoto, S., Miyamoto, T.: Development of universal vacuum gripper for wall-climbing robot. *Adv. Robot.* **32**, 283–296 (2018). <https://doi.org/10.1080/01691864.2018.1447238>
65. Fujita, M., Tadokuma, K., Komatsu, H., Takane, E., Nomura, A., Ichimura, T., Konyo, M., Tadokoro, S.: Jamming layered membrane gripper mechanism for grasping differently shaped-objects without excessive pushing force for search and rescue missions. *Adv. Robot.* **32**, 590–604 (2018). <https://doi.org/10.1080/01691864.2018.1451368>
66. Mizushima, K., Oku, T., Suzuki, Y., Tsuji, T., Watanabe, T.: Multi-fingered robotic hand based on hybrid mechanism of tendon-driven and jamming transition. In: *2018 IEEE International Conference on Soft Robotics (RoboSoft)*. pp. 376–381. *IEEE*, Livorno, Italy (2018)
67. D'Avella, S., Tripicchio, P., Avizzano, C.A.: A study on picking objects in cluttered environments: Exploiting depth features for a custom low-cost universal jamming gripper. *Robot. Comput. Integr. Manuf.* **63**, 101888 (2020). <https://doi.org/10.1016/j.rcim.2019.101888>
68. Cianchetti, M., Ranzani, T., Gerboni, G., De Falco, I., Laschi, C., Menciassi, A.: STIFF-FLOP surgical manipulator: Mechanical design and experimental characterization of the single module. In: *2013 IEEE/RSJ International Conference on Intelligent Robots and Systems*. pp. 3576–3581. *IEEE*, Tokyo, Japan (2013)
69. Jiang, P., Yang, Y., Chen, M.Z.Q., Chen, Y.: A variable stiffness gripper based on differential drive particle jamming. *Bioinspir. Biomim.* **14**, 036009 (2019). <https://doi.org/10.1088/1748-3190/ab04d1>
70. Valenzuela-Coloma, H.-R., Lau-Cortes, Y., Fuentes-Romero, R.-E., Zagal, J.C., Mendoza-Garcia, R.-F.: Mentaca: An universal jamming gripper on wheels. In: *2015 CHILEAN Conference on Electrical, Electronics Engineering, Information and Communication Technologies (CHILECON)*. pp. 817–823. *IEEE*, Santiago, Chile (2015)
71. Steltz, E., Mozeika, A., Rembisz, J., Corson, N., Jaeger, H.M.: Jamming as an enabling technology for soft robotics. In:

- Bar-Cohen, Y. (ed.) *Electroactive Polymer Actuators and Devices (EAPAD) 2010*. p. 764225 (2010)
72. Brown, E., Rodenberg, N., Amend, J., Mozeika, A., Steltz, E., Zakin, M.R., Lipson, H., Jaeger, H.M.: Universal robotic gripper based on the jamming of granular material. *Proc. Natl. Acad. Sci.* **107**, 18809–18814 (2010). <https://doi.org/10.1073/pnas.1003250107>
  73. Licht, S., Collins, E., Ballat-Durand, D., Lopes-Mendes, M.: Universal jamming grippers for deep-sea manipulation. In: *OCEANS 2016 MTS/IEEE Monterey*. pp. 1–5. IEEE, Monterey, CA, USA (2016)
  74. Li, Y., Chen, Y., Yang, Y., Wei, Y.: Passive Particle Jamming and Its Stiffening of Soft Robotic Grippers. *IEEE Trans. Robot.* **33**, 446–455 (2017). <https://doi.org/10.1109/TRO.2016.2636899>
  75. Licht, S., Collins, E., Mendes, M.L., Baxter, C.: Stronger at Depth: Jamming Grippers as Deep Sea Sampling Tools. *Soft Robot.* **4**, 305–316 (2017). <https://doi.org/10.1089/soro.2017.0028>
  76. Li, Y., Chen, Y., Li, Y.: Distributed design of passive particle jamming based soft grippers. In: *2018 IEEE International Conference on Soft Robotics (RoboSoft)*. pp. 547–552. IEEE, Livorno, Italy (2018)
  77. Licht, S., Collins, E., Badlissi, G., Rizzo, D.: A Partially Filled Jamming Gripper for Underwater Recovery of Objects Resting on Soft Surfaces. In: *2018 IEEE/RSJ International Conference on Intelligent Robots and Systems (IROS)*. pp. 6461–6468. IEEE, Madrid, Spain (2018)
  78. Li, Y., Chen, Y., Yang, Y., Li, Y.: Soft Robotic Grippers Based on Particle Transmission. *IEEE/ASME Trans. Mechatronics.* **24**, 969–978 (2019). <https://doi.org/10.1109/TMECH.2019.2907045>
  79. Yang, Y., Zhang, Y., Kan, Z., Zeng, J., Wang, M.Y.: Hybrid Jamming for Bioinspired Soft Robotic Fingers. *Soft Robot.* **7**, 292–308 (2020). <https://doi.org/10.1089/soro.2019.0093>
  80. Jiang, A., Ranzani, T., Gerboni, G., Lekstutyte, L., Althoefer, K., Dasgupta, P., Nanayakkara, T.: Robotic Granular Jamming: Does the Membrane Matter? *Soft Robot.* **1**, 192–201 (2014). <https://doi.org/10.1089/soro.2014.0002>
  81. Wall, V., Deimel, R., Brock, O.: Selective stiffening of soft actuators based on jamming. In: *2015 IEEE International Conference on Robotics and Automation (ICRA)*. pp. 252–257. IEEE, Seattle, WA, USA (2015)
  82. Ranzani, T., Gerboni, G., Cianchetti, M., Menciassi, A.: A bioinspired soft manipulator for minimally invasive surgery. *Bioinspir. Biomim.* **10**, 035008 (2015). <https://doi.org/10.1088/1748-3190/10/3/035008>
  83. Cavallo, A., Brancadoro, M., Tognarelli, S., Menciassi, A.: A Soft Retraction System for Surgery Based on Ferromagnetic Materials and Granular Jamming. *Soft Robot.* **6**, 161–173 (2019). <https://doi.org/10.1089/soro.2018.0014>
  84. Hauser, S., Mutlu, M., Freundler, F., Ijspeert, A.: Stiffness Variability in Jamming of Compliant Granules and a Case Study Application in Climbing Vertical Shafts. In: *2018 IEEE International Conference on Robotics and Automation (ICRA)*. pp. 1559–1566. IEEE, Brisbane, QLD, Australia (2018)
  85. Chopra, S., Tolley, M.T., Gravish, N.: Granular Jamming Feet Enable Improved Foot-Ground Interactions for Robot Mobility on Deformable Ground. *IEEE Robot. Autom. Lett.* **5**, 3975–3981 (2020). <https://doi.org/10.1109/LRA.2020.2982361>
  86. Amend, J.R., Brown, E., Rodenberg, N., Jaeger, H.M., Lipson, H.: A Positive Pressure Universal Gripper Based on the Jamming of Granular Material. *IEEE Trans. Robot.* **28**, 341–350 (2012). <https://doi.org/10.1109/TRO.2011.2171093>
  87. Miao, Y., Dong, W., Du, Z.: Design of a Soft Robot with Multiple Motion Patterns Using Soft Pneumatic Actuators. In: *IOP Conference Series: Materials Science and Engineering*. p. 012013. , Tianjin, China (2017)
  88. Cheng, N.G., Lobovsky, M.B., Keating, S.J., Setapen, A.M., Gero, K.I., Hosoi, A.E., Iagnemma, K.D.: Design and Analysis of a Robust, Low-cost, Highly Articulated manipulator enabled by jamming of granular media. In: *2012 IEEE International Conference on Robotics and Automation*. pp. 4328–4333. IEEE, Saint Paul, MN, USA (2012)
  89. Kapadia, J., Yim, M.: Design and performance of nubbed fluidizing jamming grippers. In: *2012 IEEE International Conference on Robotics and Automation*. pp. 5301–5306. IEEE, Saint Paul, MN, USA (2012)
  90. Jiang, Y., Amend, J.R., Lipson, H., Saxena, A.: Learning hardware agnostic grasps for a universal jamming gripper. In: *2012 IEEE International Conference on Robotics and Automation*. pp. 2385–2391. IEEE, Saint Paul, MN, USA (2012)
  91. Cheng, N., Amend, J., Farrell, T., Latour, D., Martinez, C., Johansson, J., McNicoll, A., Wartenberg, M., Naseef, S., Hanson, W., Culley, W.: Prosthetic Jamming Terminal Device: A Case Study of Untethered Soft Robotics. *Soft Robot.* **3**, 205–212 (2016). <https://doi.org/10.1089/soro.2016.0017>
  92. Harada, K., Nagata, K., Rojas, J., Ramirez-Alpizar, I.G., Wan, W., Onda, H., Tsuji, T.: Proposal of a shape adaptive gripper for robotic assembly tasks. *Adv. Robot.* **30**, 1186–1198 (2016). <https://doi.org/10.1080/01691864.2016.1209431>
  93. Fujita, M., Tadakuma, K., Takane, E., Ichimura, T., Komatsu, H., Nomura, A., Konyo, M., Tadokoro, S.: Variable inner volume mechanism for soft and robust gripping — Improvement of gripping performance for large-object gripping. In: *2016 IEEE International Symposium on Safety, Security, and Rescue Robotics (SSRR)*. pp. 390–395. IEEE, Lausanne, Switzerland (2016)
  94. Robertson, M.A., Paik, J.: New soft robots really suck: Vacuum-powered systems empower diverse capabilities. *Sci. Robot.* **2**, eaan6357 (2017). <https://doi.org/10.1126/scirobotics.aan6357>
  95. Jiang, A., Xynogalas, G., Dasgupta, P., Althoefer, K., Nanayakkara, T.: Design of a variable stiffness flexible manipulator with composite granular jamming and membrane coupling. In: *2012 IEEE/RSJ International Conference on Intelligent Robots and Systems*. pp. 2922–2927. IEEE, Vilamoura-Algarve, Portugal (2012)
  96. Athanassiadis, A.G., Miskin, M.Z., Kaplan, P., Rodenberg, N., Lee, S.H., Merritt, J., Brown, E., Amend, J., Lipson, H., Jaeger, H.M.: Particle shape effects on the stress response of granular packings. *Soft Matter* **10**, 48–59 (2014). <https://doi.org/10.1039/C3SM52047A>
  97. Wei, Y., Chen, Y., Yang, Y., Li, Y.: A soft robotic spine with tunable stiffness based on integrated ball joint and particle jamming. *Mechatronics* **33**, 84–92 (2016). <https://doi.org/10.1016/j.mechatronics.2015.11.008>
  98. A. Jiang, E. Secco, H. Wurdemann, T. Nanayakkara, K. Althoefer, P.D.: Stiffness-controllable octopus-like robot arm for minimally invasive surgery. *3rd Jt. Work. New Technol. Comput. Assist. Surg. (CRAS 2013)* Verona, Italy. (2013)
  99. Zhao, Y., Shan, Y., Zhang, J., Guo, K., Qi, L., Han, L., Yu, H.: A soft continuum robot, with a large variable-stiffness range, based on jamming. *Bioinspir. Biomim.* **14**, 066007 (2019). <https://doi.org/10.1088/1748-3190/ab3d1b>
  100. Zubrycki, I., Granosik, G.: Novel Haptic Device Using Jamming Principle for Providing Kinaesthetic Feedback in Glove-Based Control Interface. *J. Intell. Robot. Syst.* **85**, 413–429 (2017). <https://doi.org/10.1007/s10846-016-0392-6>
  101. Hauser, S., Eckert, P., Tuleu, A., Ijspeert, A.: Friction and damping of a compliant foot based on granular jamming for legged robots. In: *2016 6th IEEE International Conference on Biomedical Robotics and Biomechanics (BioRob)*. pp. 1160–1165. IEEE, Singapore (2016)

102. Hauser, S., Mutlu, M., Banzet, P., Ijspeert, A.J.: Compliant universal grippers as adaptive feet in legged robots. *Adv. Robot.* **32**, 825–836 (2018). <https://doi.org/10.1080/01691864.2018.1496851>
103. Al Abeach, L., Nefti-Meziani, S., Theodoridis, T., Davis, S.: A Variable Stiffness Soft Gripper Using Granular Jamming and Biologically Inspired Pneumatic Muscles. *J. Bionic Eng.* **15**, 236–246 (2018). <https://doi.org/10.1007/s42235-018-0018-8>
104. Thompson-Bean, E., Steiner, O., McDaid, A.: A soft robotic exoskeleton utilizing granular jamming. In: 2015 IEEE International Conference on Advanced Intelligent Mechatronics (AIM). pp. 165–170. IEEE, Busan, Korea (South) (2015)
105. Tabata, O., Konishi, S., Cusin, P., Ito, Y., Kawai, F., Hirai, S., Kawamura, S.: Micro fabricated tunable bending stiffness devices. *Sensors Actuators, A Phys.* **89**, 119–123 (2001). [https://doi.org/10.1016/S0924-4247\(00\)00538-0](https://doi.org/10.1016/S0924-4247(00)00538-0)
106. Kawamura, S., Yamamoto, T., Ishida, D., Ogata, T., Nakayama, Y., Tabata, O., Sugiyama, S.: Development of passive elements with variable mechanical impedance for wearable robots. In: Proceedings - IEEE International Conference on Robotics and Automation. pp. 248–253. IEEE, Washington, DC, USA (2002)
107. Henke, M., Sorber, J., Gerlach, G.: Multi-layer beam with variable stiffness based on electroactive polymers. In: Bar-Cohen, Y. (ed.) *Electroactive Polymer Actuators and Devices (EAPAD) 2012*. p. 83401P. SPIE, San Diego, California, United States (2012)
108. Bureau, M., Keller, T., Perry, J., Velik, R., Veneman, J.F.: Variable Stiffness Structure for limb attachment. In: 2011 IEEE International Conference on Rehabilitation Robotics. pp. 1–4. IEEE, Zurich, Switzerland (2011)
109. Kim, Y.J., Cheng, S., Kim, S., Iagnemma, K.: A novel layer jamming mechanism with tunable stiffness capability for minimally invasive surgery. *IEEE Trans. Robot.* **29**, 1031–1042 (2013). <https://doi.org/10.1109/TRO.2013.2256313>
110. Ou, J., Yao, L., Tauber, D., Steimle, J., Niiyama, R., Ishii, H.: JamSheets: Thin interfaces with tunable stiffness enabled by layer jamming. In: Proceedings of the 8th International Conference on Tangible, Embedded and Embodied Interaction - TEI '14. pp. 65–72. ACM Press, New York, New York, USA (2013)
111. Narang, Y.S., Degirmenci, A., Vlassak, J.J., Howe, R.D.: Transforming the dynamic response of robotic structures and systems through laminar jamming. *IEEE Robot. Autom. Lett.* **3**, 688–695 (2018). <https://doi.org/10.1109/LRA.2017.2779802>
112. Aktas, B., Howe, R.D.: Flexure Mechanisms with Variable Stiffness and Damping Using Layer Jamming. In: 2019 IEEE/RSJ International Conference on Intelligent Robots and Systems (IROS). pp. 7616–7621. IEEE, Macau, China (2019)
113. Zhou, Y., Headings, L.M., Dapino, M.J.: Discrete Layer Jamming for Variable Stiffness Co-Robot Arms. *J. Mech. Robot.* **12**, (2020). <https://doi.org/10.1115/1.4044537>
114. Henke, M., Gerlach, G.: On a high-potential variable-stiffness device. *Microsyst. Technol.* **20**, 599–606 (2014). <https://doi.org/10.1007/s00542-013-1995-5>
115. Choi, Y.T., Hartzell, C.M., Leps, T., Wereley, N.M.: Gripping characteristics of an electromagnetically activated magnetorheological fluid-based gripper. *AIP Adv.* **8**, 056701 (2018). <https://doi.org/10.1063/1.5006094>
116. Białek, M., Jędrzycka, C., Milecki, A.: Investigation of thermo-plastic polyurethane finger cushion with magnetorheological fluid for soft-rigid gripper. *Energies*. **14**, (2021). <https://doi.org/10.3390/en14206541>
117. Guo, J., Bamber, T., Hovell, T., Chamberlain, M., Justham, L., Jackson, M.: Geometric Optimisation of Electroadhesive Actuators Based on 3D Electrostatic Simulation and its Experimental Verification. *IFAC-PapersOnLine*. **49**, 309–315 (2016). <https://doi.org/10.1016/j.ifacol.2016.10.574>
118. Yatsuzuka, K., Hatakeyama, F., Asano, K., Aonuma, S.: Fundamental characteristics of electrostatic wafer chuck with insulating sealant. *IEEE Trans. Ind. Appl.* **36**, 510–516 (2000). <https://doi.org/10.1109/28.833768>
119. Higham, T.E., Russell, A.P., Niewiarowski, P.H., Wright, A., Speck, T.: The Ecomechanics of Gecko Adhesion: Natural Surface Topography, Evolution, and Biomimetics. *Integr. Comp. Biol.* **59**, 148–167 (2019). <https://doi.org/10.1093/icb/icz013>
120. Asano, K., Hatakeyama, F., Yatsuzuka, K.: Fundamental study of an electrostatic chuck for silicon wafer handling. *IEEE Trans. Ind. Appl.* **38**, 840–845 (2002). <https://doi.org/10.1109/TIA.2002.1003438>
121. Chen, R.: A Gecko-Inspired Electroadhesive Wall-Climbing Robot. *IEEE Potentials* **34**, 15–19 (2015). <https://doi.org/10.1109/MPOT.2014.2360020>
122. Owano, N.: Grabit uses electroadhesion for good grip on objects. <https://techxplore.com/news/2014-10-grabit-electroadhesion-good.html>
123. Shintake, J., Rosset, S., Schubert, B., Floreano, D., Shea, H.: Versatile Soft Grippers with Intrinsic Electroadhesion Based on Multifunctional Polymer Actuators. *Adv. Mater.* **28**, 231–238 (2016). <https://doi.org/10.1002/adma.201504264>
124. Monkman, G.J., Taylor, P.M., Farnworth, G.J.: PRINCIPLES OF ELECTROADHESION IN CLOTHING ROBOTICS. *Int. J. Cloth. Sci. Technol.* **1**, 14–20 (1989). <https://doi.org/10.1108/eb002951>
125. Zhou, M., Pesika, N., Zeng, H., Tian, Y., Israelachvili, J.: Recent advances in gecko adhesion and friction mechanisms and development of gecko-inspired dry adhesive surfaces. *Friction*. **1**, 114–129 (2013). <https://doi.org/10.1007/s40544-013-0011-5>
126. Aksak, B., Murphy, M.P., Sitti, M.: Adhesion of Biologically Inspired Vertical and Angled Polymer Microfiber Arrays. *Langmuir* **23**, 3322–3332 (2007). <https://doi.org/10.1021/la062697t>
127. Hawkes, E.W., Eason, E.V., Christensen, D.L., Cutkosky, M.R.: Human climbing with efficiently scaled gecko-inspired dry adhesives. *J. R. Soc. Interface*. **12**, 20140675 (2015). <https://doi.org/10.1098/rsif.2014.0675>

**Publisher's Note** Springer Nature remains neutral with regard to jurisdictional claims in published maps and institutional affiliations.

Springer Nature or its licensor (e.g. a society or other partner) holds exclusive rights to this article under a publishing agreement with the author(s) or other rightsholder(s); author self-archiving of the accepted manuscript version of this article is solely governed by the terms of such publishing agreement and applicable law.

**Kunal Singh** received his B.Tech and M.Tech degrees in mechanical engineering from Kurukshetra University, Kurukshetra, India, and Thapar University, Patiala, India in 2009 and 2012. He is currently pursuing a Ph.D. in soft robotics and his research interest includes 3D printing, sensors, actuators, and bio-inspired robots.

**Shilpa Gupta** received her B.Tech. degree in electronics and communication engineering from the Kurukshetra University, India, in 2002, M.Tech in 2009, and a Ph.D. degree in 2020 in electrical engineering from the National Institute of Technology, Kurukshetra, India, respectively. Her current research interests include soft robotics, sensors, actuators, reliability, multistage interconnection networks, and parallel computing.